

Oxidation of Mercury Across SCR Catalysts in Coal-Fired Power Plants Burning Low Rank Fuels

Final Report

Period of Performance: February 19, 2003 to September 30, 2004

Constance Senior

December 31, 2004

DOE Cooperative Agreement No: DE- FC26-03NT41728

Reaction Engineering International
77 West 200 South, Suite 210
Salt Lake City, UT 84101

Disclaimer

“This report was prepared as an account of work sponsored by an agency of the United States Government. Neither the United States Government nor any agency thereof, nor any of their employees, makes any warranty, express or implied, or assumes any legal liability or responsibility for the accuracy, completeness, or usefulness of any information, apparatus, product, or process disclosed, or represents that its use would not infringe privately owned rights. Reference herein to any specific commercial product, process, or service by trade name, trademark, manufacturer, or otherwise does not necessarily constitute or imply its endorsement, recommendation, or favoring by the United States Government or any agency thereof. The views and opinions of authors expressed herein do not necessarily state or reflect those of the United States Government or any agency thereof.”

Abstract

The objectives of this program were to measure the oxidation of mercury in flue gas across SCR catalyst in a coal-fired power plant burning low rank fuels using a slipstream reactor containing multiple commercial catalysts in parallel and to develop a greater understanding of mercury oxidation across SCR catalysts in the form of a simple model. The Electric Power Research Institute (EPRI) and Argillon GmbH provided co-funding for this program. REI used a multicalyst slipstream reactor to determine oxidation of mercury across five commercial SCR catalysts at a power plant that burned a blend of 87 % subbituminous coal and 13 % bituminous coal. The chlorine content of the blend was 100 to 240 $\mu\text{g/g}$ on a dry basis. Mercury measurements were carried out when the catalysts were relatively new, corresponding to about 300 hours of operation and again after 2,200 hours of operation. NO_x , O_2 and gaseous mercury speciation at the inlet and at the outlet of each catalyst chamber were measured. In general, the catalysts all appeared capable of achieving about 90% NO_x reduction at a space velocity of 3,000 hr^{-1} when new, which is typical of full-scale installations; after 2,200 hours exposure to flue gas, some of the catalysts appeared to lose NO_x activity. For the fresh commercial catalysts, oxidation of mercury was in the range of 25 % to 65 % at typical full-scale space velocities. A blank monolith showed no oxidation of mercury under any conditions. All catalysts showed higher mercury oxidation without ammonia, consistent with full-scale measurements. After exposure to flue gas for 2,200 hours, some of the catalysts showed reduced levels of mercury oxidation relative to the initial levels of oxidation. A model of Hg oxidation across SCRs was formulated based on full-scale data. The model took into account the effects of temperature, space velocity, catalyst type and HCl concentration in the flue gas.

Table of Contents

<i>Executive Summary</i>	<i>1</i>
<i>Experimental Methods</i>	<i>3</i>
Task 3 – Field Measurements and Mercury Speciation	3
Site Description	3
Slipstream Reactor Description	3
First Test Series	6
Second Test Series	8
Task 4 - Data Analysis and Validation	9
<i>Results and Discussion</i>	<i>10</i>
Task 3 – Field Measurements and Mercury Speciation	10
Coal and Ash Data	10
NO _x Performance	16
Mercury Speciation Data	19
Task 4 - Data Analysis and Validation	35
<i>Conclusions</i>	<i>45</i>
<i>Acknowledgements</i>	<i>45</i>
<i>References</i>	<i>46</i>
<i>Appendix A</i>	<i>47</i>
<i>Appendix B</i>	<i>50</i>
<i>Appendix C</i>	<i>56</i>

List of Tables

Table	Page
Table 1. Catalyst Properties	3
Table 2. Measurements and samples collected during first test series.	7
Table 3. Measurements and samples collected during second test series.	8
Table 4. Coal analyses from first test series.	10
Table 5. Ash composition: Major elements as wt% oxides, SO ₃ -free basis.	11
Table 6. Flue gas composition estimated from coal composition for first test series.	12
Table 7. Coal analyses from second test series.	13
Table 8. Composition of ash collected from ESP hoppers (second test series).	14
Table 9. Flue gas composition estimated from coal composition for second test series, except as noted; coal moisture content adjusted to 26.5%.	15
Table 10. Results of halide measurements in gas, corrected to 5% O ₂ (wet basis).	16
Table 11. Relationship between NO _x reduction and temperature from August test data.	18
Table 12. Ontario Hydro measurements for first test series (28 March 2003); mercury concentrations in µg/Nm ³ at 5% O ₂ .	20
Table 13. Ontario Hydro measurements for second test series, corrected to 5% O ₂ .	21
Table 14. Inlet Mercury concentrations measured by various methods in second test series.	22
Table 15. Flue gas compositions used for equilibrium calculations.	39
Table 16. Rate constants derived from full-scale data.	42

List of Figures

Figure	Page
Figure 1. Arrangement of catalysts in slipstream reactor (plan view).	4
Figure 2. Schematic of slipstream reactor.	5
Figure 3. Field setup of the SCEM and impingers.	6
Figure 4. Mercury remaining in Eagle Butte subbituminous coal after thermal treatment.	13
Figure 5. Coal mercury content as a function of sample date.	14
Figure 6. NO _x reduction as a function of space velocity for commercial catalysts from March/April for excess ammonia and catalyst temperatures in the range of 620-650°F.	17
Figure 7. NO _x reduction as a function of NH ₃ /NO ratio for commercial catalysts from August; temperatures (in degrees F) and space velocities (in hr ⁻¹).	17
Figure 8. NO _x reduction as a function of temperature for commercial catalysts from August; NH ₃ /NO ratios and space velocities (in hr ⁻¹).	18
Figure 9. NO _x reduction as a function of space velocity for commercial catalysts from March/April for excess ammonia and catalyst temperatures in the range of 620-650°F compared with August data (extrapolated to the appropriate temperature range).	19
Figure 10. Total mercury measurements, μg/Nm ³ for first test series, corrected to 5% O ₂ .	20
Figure 11. Mercury SCEM data (μg/Nm ³ at 5% O ₂) for elemental mercury at 3000-7000 hr ⁻¹ space velocity with NH ₃ /NO=5.	23
Figure 12. Average values of mercury SCEM data (μg/Nm ³ at 5% O ₂) for elemental mercury at 3000-7000 hr ⁻¹ space velocity with NH ₃ /NO=5.	24
Figure 13. Calculated loss of total mercury across for the first test series catalyst chambers for space velocity of 2,000-5,000 hr ⁻¹ , with and without ammonia (NH ₃ /NO=2.4).	24
Figure 14. Loss of total mercury across commercial catalysts as a function of time since last start-up of reactor for the first test series.	25

Figure	Page
Figure 15. Loss of total mercury across commercial catalysts for the first test series as a function of oxidized mercury at outlet (estimated from separate elemental mercury measurements).	26
Figure 16. Total Mercury as a function of time from second test series, space velocity 2,500-5,000 hr ⁻¹ , NH ₃ /NO=1, 555-600°F.	27
Figure 17. Oxidation (net loss of elemental mercury) in the first test series at 650°F as a function of space velocity for excess ammonia (NH ₃ /NO: 1.2-2.0).	28
Figure 18. Estimated loss of elemental mercury in the first test series across catalyst chambers for space velocity of 2,500 hr ⁻¹ , with and without ammonia (NH ₃ /NO=1.2-2.0).	29
Figure 19. SCEM measurements of elemental mercury during the second test series at SV=2000-5000 hr ⁻¹ and NH ₃ /NO=0.94-1.2: (a) August 12 and (b) August 13.	30
Figure 20. Mercury oxidation as a function of space velocity for NH ₃ /NO = 0.9-1.2.	31
Figure 21. Comparison of mercury oxidation from the first test series (NH ₃ /NO: 1.2-2.0) and the second test series (NH ₃ /NO: 0.9-1.2) with ammonia: (a) monolith catalysts and (b) plate catalysts.	31
Figure 22. Elemental mercury during second test series, SV=2000-4000 hr ⁻¹ .	32
Figure 23. Mercury oxidation with and without ammonia estimate at 2,500 hr ⁻¹ ; March/April test series: NH ₃ /NO=1.2-2.0; August test series: NH ₃ /NO=0.9-1.2.	32
Figure 24. Elemental mercury and NO _x as a function of time for catalyst C2; T=550°F, SV=5,100 hr ⁻¹ .	33
Figure 25. Elemental mercury and NO _x as a function of time for catalyst C5; T=600°F, SV=7,000 hr ⁻¹ , NH ₃ /NO=1.2 or T=540°F, SV=2,600 hr ⁻¹ , NH ₃ /NO=3.75.	34
Figure 26. Elemental mercury and NO _x as a function of time for catalyst C3; T=574 F, SV=1,110 hr ⁻¹ , NH ₃ /NO=3.44.	35
Figure 27. Change in elemental mercury across full-scale SCRs compared with change in oxidized mercury.	37
Figure 28. Mercury speciation from thermochemical equilibrium calculations for flue gas compositions from Table 15.	38

Figure	Page
Figure 29. Percentage of mercury as elemental at inlet to SCR: full-scale data compared to equilibrium predictions.	39
Figure 30. Percentage of mercury as elemental at outlet to SCR: full-scale data compared to equilibrium predictions.	39
Figure 31. Mercury oxidation across full-scale SCRs as a function of inlet temperature.	40
Figure 32. Mercury oxidation across full-scale SCRs as a function of coal chlorine content.	40
Figure 33. $\frac{W[HCl][Hg^0]_{in}}{F_{in}}$ vs. $\ln\left(\frac{1}{1-X}\right)$ from full-scale data with ammonia.	42
Figure 34. $\frac{W[HCl][Hg^0]_{in}}{F_{in}}$ vs. $\ln\left(\frac{1}{1-X}\right)$ from full-scale data with and without ammonia, 667-681°F.	43
Figure 35. Calculated Hg oxidation across full-scale SCRs.	44

Executive Summary

Selective Catalytic Reduction (SCR) is being used on U.S. coal-fired power plants for the control of NO_x emissions. Gaseous mercury has been observed to be highly oxidized downstream of SCR systems in full-scale power plants. Pilot-scale and slipstream investigations have shown that mercury oxidizes across SCR catalysts and that flue gas from bituminous coals shows more oxidation than that from subbituminous coals. In this program, REI used a mult catalyst slipstream reactor to determine oxidation of mercury at AEP's Rockport Unit 1, a plant that burns a blend of 87 % subbituminous coal and 13 % bituminous coal. This project received funding from the Department of Energy under Cooperative Agreement No: DE-FC26-03NT41728. The Electric Power Research Institute (EPRI) and Argillon GmbH provided co-funding for this program. The period of performance was from February 19, 2003 through September 30, 2004.

Under a separate program (cooperative agreement DE-FC26-00NT40753), Reaction Engineering International (REI) was funded by the Department of Energy to carry out research and development on NO_x control options for coal-fired utility boilers. The objective of one of the tasks in the NO_x-control program was to evaluate and model SCR catalyst deactivation. REI carried out long-term testing of multiple commercial catalysts simultaneously in a power plant slipstream reactor. This multi-catalyst reactor provided an ideal test bed for advancing the state of knowledge regarding mercury oxidation by SCR catalysts, with a focus on low rank fuels.

During the six-month testing under the existing NO_x-control program, two week-long sampling campaigns for mercury speciation were carried out: at the beginning of the six-month period and at an intermediate point. URS conducted the one-week campaigns to measure gaseous mercury speciation at the inlet and at the outlet of each catalyst chamber.

Five commercial catalysts and one blank monolith were exposed to flue gas. Mercury measurements were carried out when the catalysts were relatively new, corresponding to about 300 hours of operation, and again after 2,200 hours of operation. NO_x, O₂ and gaseous mercury speciation at the inlet and at the outlet of each catalyst chamber were measured. In general, the catalysts all appeared capable of achieving about 90% NO_x reduction at a space velocity of 3,000 hr⁻¹ when new, which is typical of full-scale installations; after 2,200 hours exposure to flue gas, some of the catalysts appeared to lose NO_x activity. Fresh commercial catalysts showed mercury oxidation that was in the range of 25 % to 65 % at typical full-scale space velocities, consistent with observed full-scale oxidation in bituminous coal flue gas, even though the blend was predominantly subbituminous coal. However, the chlorine content of the blend (100 to 240 µg/g on a dry basis) was higher than typical values for subbituminous coals. A blank monolith showed no oxidation of mercury under any conditions. All catalysts showed higher mercury oxidation without ammonia, consistent with full-scale measurements. After exposure to flue gas for 2,200 hours, some of the catalysts showed reduced levels of mercury oxidation relative to the initial levels of oxidation.

A review of the available data on mercury oxidation across SCR catalysts from small, laboratory-scale experiments, pilot-scale slipstream reactors and full-scale power plants was carried out. SCR catalysts are, under certain circumstances, capable of driving mercury speciation toward the gas-phase equilibrium values at the SCR temperature. However, evidence suggests that mercury does not reach equilibrium at the outlet of SCR catalysts. Some of the

2

other factors that have been shown to affect mercury chemistry across SCR catalysts are the space velocity and the presence of ammonia. There may be other factors, such as the sulfur content of the coal, that become apparent as more data become available. Catalyst properties may be important, including: the mix between vanadium oxides and other oxides in the catalyst; the pore size distribution; and catalyst deactivation with time.

A global kinetic model of Hg oxidation across SCRs was formulated based on full-scale data. The model took into account the effects of temperature, space velocity, catalyst type and HCl concentration in the flue gas. The results of this analysis suggest strategies for maximizing the amount of oxidized mercury at the exit of SCR catalysts. The chief of these is to increase the chlorine content of the flue gas, either through blending low-chlorine coal with high-chlorine coal or additives. Lowering the temperature is another option, but this may not be practical in many utility boilers. Furthermore, NO reduction across SCR catalysts decreases with temperature.

Experimental Methods

Within this section we present in order, brief discussions on the different tasks that are contained within this program. For simplicity, the discussion items are presented in the order of the Tasks as outlined in the original proposal.

Task 3 – Field Measurements and Mercury Speciation

Site Description

The Rockport plant consists of two 1300 MW_e B&W opposed wall-fired boilers. These are supercritical boilers that burn a blend of bituminous and subbituminous coals. The average mix was 87% Powder River Basin (PRB) subbituminous and 13% eastern bituminous coal. The plant had a cold-side electrostatic precipitator (ESP).

Mercury measurements were carried out March 28-April 2, 2003 and August 7 to 16, 2003. At the time of the first test series (March/April) the catalysts had been exposed to flue gas for approximately 300 hours. At the time of the second test series (August) the catalyst had been exposed to flue gas for approximately 2,200 hours.

Slipstream Reactor Description

The slipstream reactor was conceived and built to test the deactivation of SCR catalysts in the field. The reactor contained six SCR catalysts in parallel and was designed to withdraw a flue gas sample at the exit of the economizer. The reactor contained five commercial catalysts, both plate and honeycomb monolith type, and one blank cordierite monolith. The commercial monolith catalysts had approximately a 7 mm pitch. The blank monolith had a slightly smaller pitch of 3.6 mm. Details of the catalysts' physical properties are given in Table 1. The six catalysts, four monolith and two plate, were configured (in plan view) as shown in Figure 1.

Table 1. Catalyst Properties.

Chamber:	C1 (Blank)	C2	C3	C4	C5	C6
Catalyst type	Monolith	Monolith	Plate	Plate	Monolith	Monolith
Catalyst pitch (mm)	3.6	7.1	5.7	5.7	7.0	7.4
Chamber porosity	58.7%	75.4%	83.4%	85.1%	70.0%	67.6%
Length of catalyst in chamber (m)	0.62	0.55	1.09	1.00	0.49	0.50
Volume of catalyst block (m ³)	0.0064	0.0057	0.0130	0.0135	0.0057	0.0056

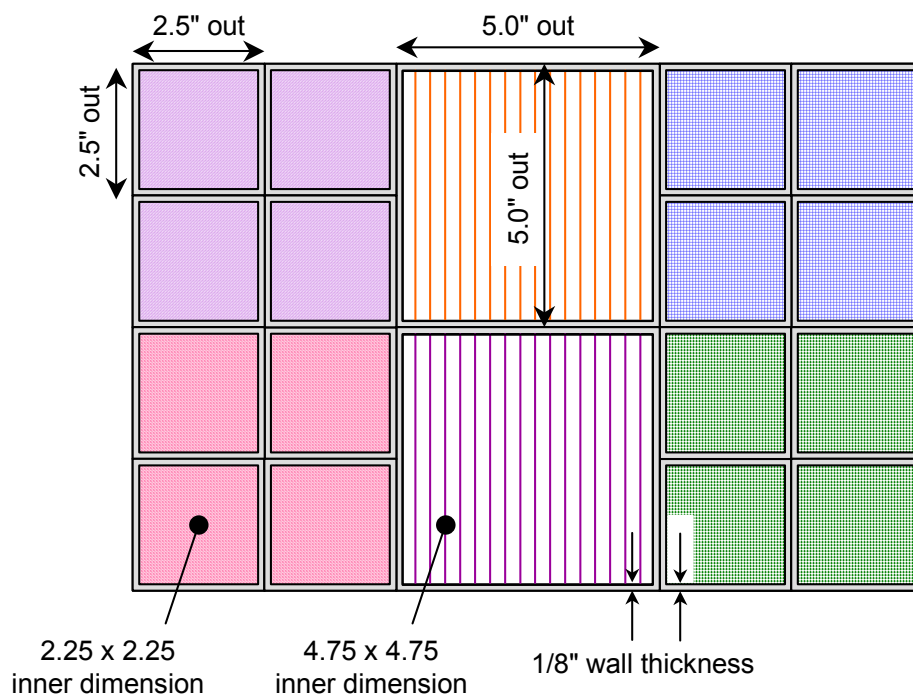


Figure 1. Arrangement of catalysts in slipstream reactor (plan view).

Figure 2 is a schematic of the slipstream SCR reactor as installed on Unit 1. An inlet probe was inserted through an existing port in the duct wall upstream of one of the air preheaters. An isolation valve was placed on the inlet line just outside the duct wall. The probe extended approximately three feet into the duct and had a two-foot long slot, oriented 90 degrees from the direction of flow in the duct. Unlike previous slipstream reactors for SCR catalyst testing (for example, Reference 7), the catalysts were exposed to fly ash during the test period. As shown in Figure 2, the slipstream reactor was fitted with a three-inch port for Ontario Hydro measurements, one SCR inlet heated sample line and an outlet heated sample line for each of the six catalyst chambers. Anhydrous ammonia was injected into the flue gas stream near the entrance to the reactor, and blended into the flue gas with a static mixer.

Control of flow through the test chambers was achieved using eductors on each chamber; the compressed air flow to the eductors was regulated by the control system, based on the desired set points. Because the flow rates needed for the mercury testing were about ten times lower than those needed for the catalyst deactivation experiments, modifications were made to the operation of the system to achieve those flow rates. The manual gate valve on the outlet of the reactor was partially closed, which restricted the flow through the reactor and increased the pressure. This allowed the eductors to control flow in the desired range. This method promoted ash build-up in the reactor, however. During the tests, some of the catalyst chambers became blocked and had to be cleaned. During the tests, problems were also experienced with limitation of flow rates from the catalyst chambers caused by blocked ash filters. This was manifested by high oxygen content in the gas being sampled by the semi-continuous mercury emissions monitor (SCEM), indicating that the sample pump was pulling in outside air because of the partial blockage of the ash filters.

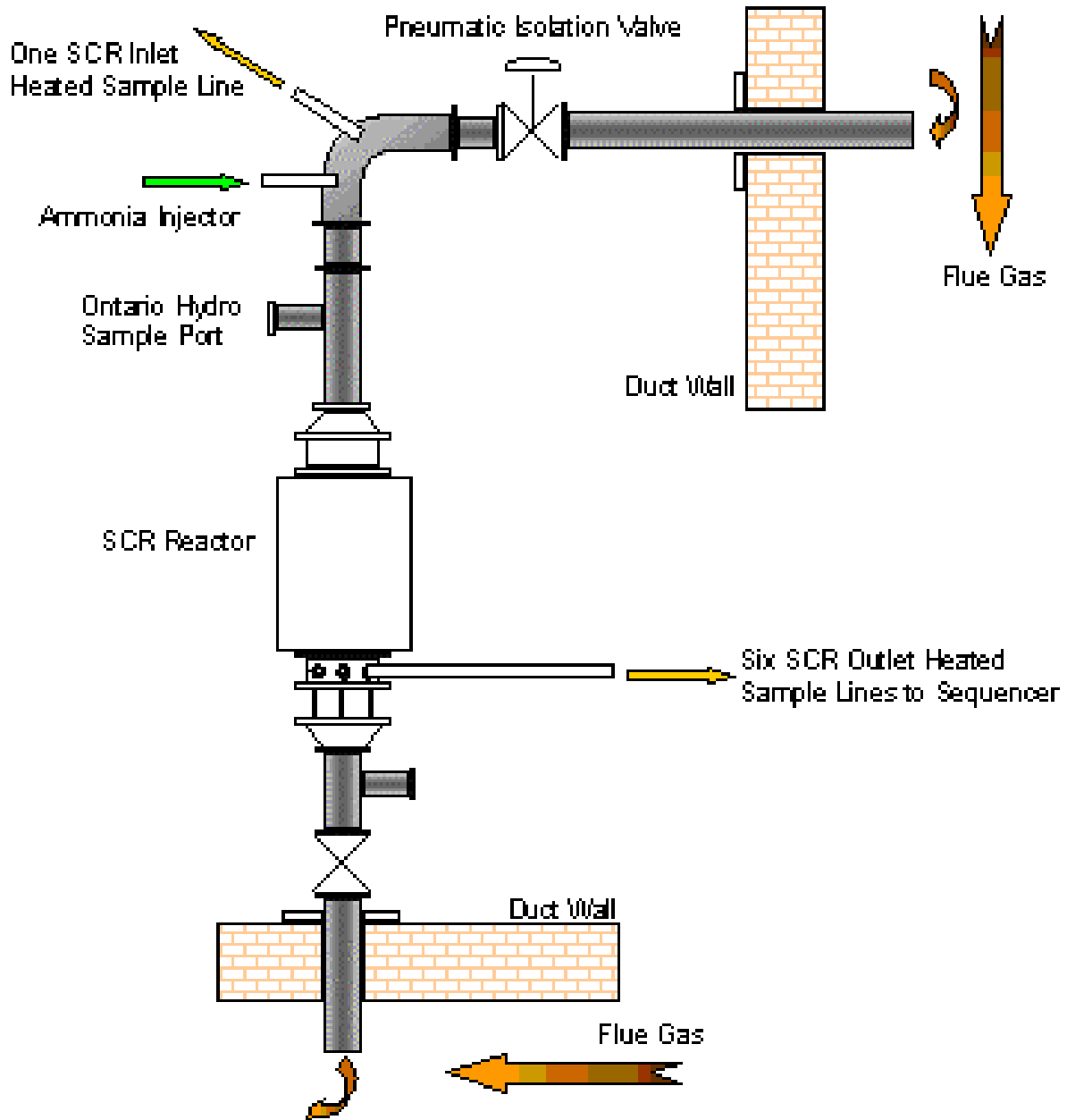


Figure 2. Schematic of slipstream reactor.

The system had seven sampling ports, one before the catalyst chambers and one after each of the six catalyst sections. The ports themselves consisted of thin stainless steel tubes that enter the channel and bend downward, in line with gas flow. There were sintered metal filters at the point where the individual samples were withdrawn; these could be blown back with compressed air. The inlet sample had a 30-foot, one-quarter-inch stainless steel heated line (upstream of the sample conditioning unit); the six outlet samples had 10-foot, one-quarter-inch stainless steel heated lines. The sample lines were heated to about 120°C (250°F).

For the SCEM measurements, a sample gas from the sequencer was directed to a train of impingers (see Figure 3). For elemental mercury measurement, the flue gas was passed through impingers containing potassium chloride solution (KCl) followed by a set of impingers containing caustic soda, NaOH. KCl captured oxidized mercury while allowing elemental mercury to flow through. NaOH was used for removing acid gases in the flue gas (SO_2 , HCl). For total mercury measurements, the KCl impingers were replaced with a set of impingers containing stannous chloride (SnCl_2). Stannous chloride reduced oxidized mercury to elemental mercury. Thus downstream mercury measurement equipment detected total mercury in the sample gas (elemental mercury + oxidized mercury).

After passing through the impingers, the flue gas was directed to an amalgamation unit (gold trap) that adsorbs mercury at a temperature slightly below room temperature. After a predetermined amount of time, the gold trap is heated to release the concentrated mercury, which is conveyed in a carrier gas to a cold-vapor atomic adsorption accessory for quantitative analysis.

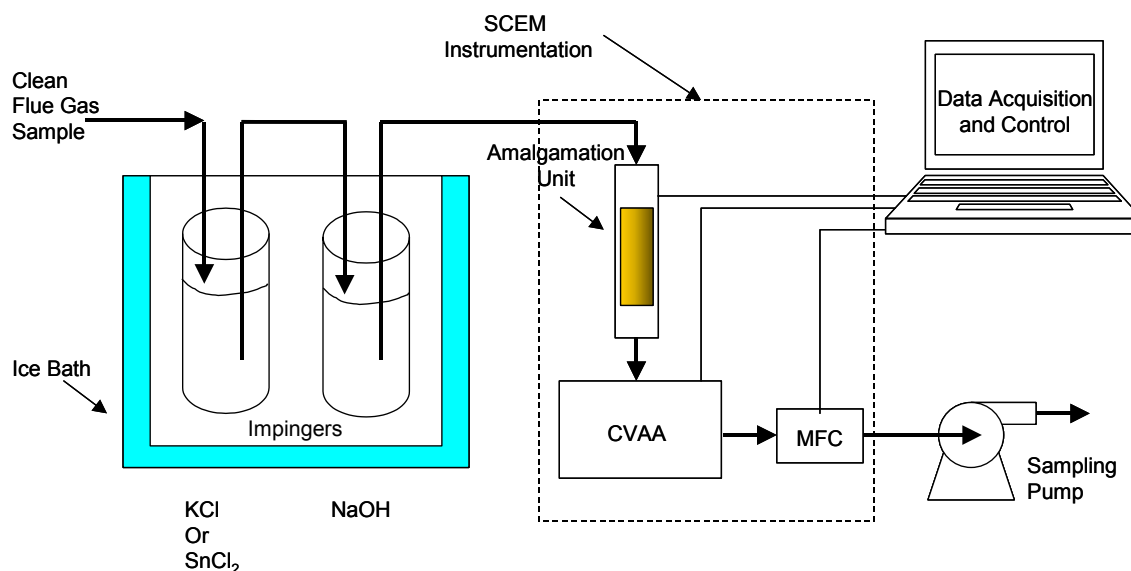


Figure 3. Field setup of the SCEM and impingers.

First Test Series

Mercury measurements were taken during March 28 through April 2, 2003. At the time of the mercury measurements, the catalysts had been exposed to flue gas for approximately 300 hours. Prior to beginning the test, the reactor was taken off-line for ash removal for several days. Therefore, at the start of the mercury measurements, the catalyst had not been exposed to flue gas for several days

During the tests, the temperature in the boiler duct was approximately 385°C (720°F). Temperature in the catalyst chambers was controlled to 345°C (650°F), using strip-heaters and based on thermocouples located on the outside of the chambers. Stable flow and temperature conditions were generally achieved. The ammonia flow was calculated assuming that the NO

concentration in the flue gas was 400 ppm because the NO_x analyzer was not on line during the mercury testing. NO_x measurements made after the mercury sampling indicated the average NO_x concentration was approximately 330 ppm (wet basis, 5% O₂).

There were six catalyst chambers consisting of two plate-type catalysts and four monolith (honeycomb) catalysts as discussed above. The sampling was controlled automatically by the slipstream reactor control system; the sequence was: inlet, chamber one, chamber two, chamber three, inlet, chamber four, chamber five, chamber six, inlet. Tests conducted on the first day employed thirty-minute sampling times for each sample line. In subsequent tests, the sampling time was limited to twenty minutes.

The sample gases were routed through the sample conditioning and switching unit: seven lines came in from the reactor and one line went out either to the NO_x/O₂ analyzer or to the mercury SCEM. The switching valves were in a heated box, heated to 80°C (175°F). There was blowback air for these valves. Problems were encountered with plugging of ash on the sintered metal filters; the sample lines had to be blown back before each sample.

Table 2 shows a list of samples collected during the tests for further analysis. During the test run on March 28, 2003 both the Ontario Hydro and the SCEM were run simultaneously. The Ontario Hydro sample was taken through the three-inch port upstream of the catalyst chambers indicated in Figure 2. Analysis of the Ontario Hydro filters and impinger solutions was carried out by URS.

Table 2. Measurements and samples collected during first test series.

Parameter	Sample/Signal/Test	Frequency
Coal	Batch sample to pulverizer, as fired. Ultimate, proximate, ash composition, Hg, Cl analyses.	Daily
Fly ash	Batch sample from ESP silos 3 & 4 and from economizer hopper. LOI, Hg, Cl, ash composition analyses.	Daily
Unit operation	Plant PI Data: Boiler load Flow rates and temperatures O ₂ (air preheater) NO _x , SO ₂ (stack)	At least several times per day
Mercury (total and speciated)	Inlet and outlet of catalyst chambers (SCEM)	Per test plan
Mercury (total and speciated)	Ontario Hydro, inlet of APH	Once, three repeat measurements

Coal samples were taken at the inlet to the pulverizers during the testing, as were ESP hopper ash samples and economizer hopper ash samples. Coal and ash samples were analyzed by Microbeam Technologies, Inc. (Grand Forks, ND). To minimize fluctuations in mercury in the flue gas, the plant was run at constant load throughout the mercury measurement periods.

Second Test Series

The second test series was begun at the beginning of August; data were taken between August 7 and August 16, 2003. The test crew from URS used a semi-continuous mercury emissions monitor to provide near real-time feedback during catalyst evaluations. To minimize fluctuations in mercury in the flue gas, the plant was run at constant load throughout the mercury measurement periods.

During the tests, the temperature in the boiler duct was approximately 730-745°F. Temperature in the catalyst chambers was controlled to 600°F, based on thermocouples located on the outside of the chambers. Stable flow and temperature conditions were generally achieved. During the second test series, there was difficulty in getting sufficient power to the heaters around the catalyst chambers. Temperatures in the chambers were somewhat lower than in the first test series because of problems with the external heaters for the catalyst chambers. Table 3 shows a summary of the test conditions and samples taken.

Table 3. Measurements and samples collected during second test series.

Date	Measurements at Reactor	Sample	Analyses
8/7/2003	SCEM: Total Hg at inlet and through Chamber 1 (Blank) SCEM: Inlet Elemental Hg Two out of three Ontario Hydro measurements	Coal: Mills 1&2, 6&7 Fly Ash 3&4	Ult/prox, Hg, Cl LOI, Hg, Cl
8/8/2003	SCEM: Total Hg at inlet One out of three Ontario Hydro measurements Gas-phase halide measurement	Coal: Mills 1&2, 6&7 Fly Ash 3&4	Ult/prox, Hg, Cl
8/10/2003		Coal: Mills 1&2, 6&7 Fly Ash 3&4	Ult/prox, Hg, Cl
8/11/2003	SCEM: Total Hg at inlet and outlet of chambers	Coal: Mills 1&2, 6&7 Fly Ash 3&4 Economizer Ash	Ult/prox, Hg, Cl LOI, Hg, Cl LOI, Hg, Cl
8/12/2003	SCEM: Elemental Hg at inlet and outlet of chambers SCEM: Total Hg at inlet	Coal: Mills 1&2, 6&7 Fly Ash 3&4	Ult/prox, Hg, Cl
8/13/2003	SCEM: Elemental Hg at inlet and outlet of chambers SCEM: Total Hg at inlet	Coal: Mills 1&2, 6&7 Fly Ash 3&4	Ult/prox, Hg, Cl
8/15/2003	SCEM: Elemental Hg at inlet and outlet of chambers, transient SCEM: Total Hg at inlet	Coal: Mills 1&2, 6&7 Fly Ash 3&4 Economizer Ash	Ult/prox, Hg, Cl LOI, Hg, Cl LOI, Hg, Cl
8/16/2003	SCEM: Elemental Hg at inlet and outlet of chambers, transient SCEM: Total Hg at inlet	Coal: Mills 1&2, 6&7 Fly Ash 3&4	Ult/prox, Hg, Cl

Coal and ash samples were analyzed by Microbeam Technologies, Inc. (Grand Forks, ND). During the testing on August 7 and 8 both the Ontario Hydro and the SCEM were run simultaneously. The Ontario Hydro sample was taken through the three-inch port upstream of the catalyst chambers indicated in Figure 2. SCEM measurements were made through the individual sample lines, as discussed below. Carbon trap measurements and gaseous halide measurements were made at the SCEM sampling point, too. The gaseous halide measurements were made using impingers designed to separate HCl/HF from Cl_2/F_2 . Analysis of the Ontario Hydro filters and impinger solutions, carbon traps, and halide impinger solutions was carried out by URS.

There was concern after the first test series that the heated switching valve box was too cold and this might result in loss of oxidized mercury, which could explain the apparent loss of total mercury across the catalysts observed in the first test series. The temperature of the heated switching box was turned up, but this caused one of the components to fail. Even after the manufacturer repaired the switching box, ash plugging in the switching box remained a problem. Therefore, the sample lines were individually and manually connected to URS's inertial separation probe for most of the second test series. This is a heated stainless steel probe that has taps to withdraw small sample flows. Gas passing through the sample taps first passes through a sintered metal tube, providing another stage of filtering. Using the inertial separation probe reduced the ash pluggage, but increased the sample time because the sample lines had to be manually disconnected, blown out with air and then reconnected for each sample.

Task 4 - Data Analysis and Validation

Laboratory¹⁻³ and pilot-scale⁴⁻⁷ data have been collected on the behavior of mercury in SCR catalysts, in addition to the pilot-scale data obtained in this program. Data have been collected from measurements of mercury speciation across SCRs in six full-scale power plants under funding by DOE NETL and EPRI^{8,9}, from other utility data and from other data reported in the literature.¹⁰ Appendix A provides details of the design and operating conditions, and the measured mercury speciation and oxidation in these catalysts. Further information can be found in References 8 through 10. The ammonia-to-NO ratios for these full-scale systems are not given; however, since the full-scale data all come from operating electric utility boilers, the NO_x reductions achieved by the SCR catalysts would be of a similar magnitude.

Results and Discussion

Task 3 – Field Measurements and Mercury Speciation

Coal and Ash Data

Table 4 presents the coal data on an as-received basis from the first test series. The coal blend was nominally 87% PRB subbituminous and 13% eastern bituminous. The heating value of the coal was commensurate with the blend, as was the coal chlorine content. The mercury content of the coal was equivalent to 8 to 11 $\mu\text{g}/\text{nm}^3$ of mercury, if all the mercury were in the flue gas at 5% O_2 .

Table 4. Coal analyses from first test series.

Date	3/28/03	4/1/03	4/2/03
ULTIMATE ANALYSIS (As Received):			
Carbon	50.67	51.80	51.75
Hydrogen	3.51	3.64	3.46
Oxygen	10.89	11.04	11.18
Nitrogen	0.76	0.78	0.75
Sulfur	0.32	0.30	0.37
Ash	5.12	5.99	6.10
Moisture	28.74	26.45	26.39
HHV, Btu/lb	8,723	8,989	8,989
Hg, $\mu\text{g}/\text{g}$, dry basis	0.0881	0.118	0.0911
Cl, $\mu\text{g}/\text{g}$, dry basis	120	160	200
SO_2 , lb/MBtu	0.74	0.67	0.82
Hg, lb/TBtu	7.20	9.66	7.46
Hg, $\mu\text{g}/\text{dnm}^3$ (5% O_2)	8.02	10.82	8.46

The ash composition of the coal was measured using the standard ASTM Ash Chemistry method. This composition is shown in Table 4 for one day, calculated on an SO_3 -free basis. The ash compositions were also measured in the economizer ash and the ESP ash; these are shown for comparison with the coal ash in Table 4. As expected from the blend, the ash contained significant calcium (about 16 wt% as CaO) and more iron than might be found in a typical Powder River Basin subbituminous coal. The sodium content of coal was about 1.5 wt% Na_2O .

Ash samples were analyzed for loss on ignition (LOI), Hg and Cl, as shown in Table 5. The LOI of these samples was generally low. Since the ash was a pale tan color, the carbon content of the ash was probably even lower than indicated by the LOI

values. In any case, the ash had a very low amount of unburned carbon. The ESP ash had 15 to 20 times more mercury than the economizer ash sample; this suggests that there was some adsorption of mercury by the ash that took place between the economizer and the ESP (probably post-air preheater). However, the amount of mercury adsorbed on the ESP ash was less than 0.5% of the mercury in the coal. Thus, the fly ash from Rockport was very unreactive toward mercury.

The chlorine content of the ash was fairly constant from the economizer to the ESP sample, suggesting that any reaction of gaseous chlorine compounds with ash took place at temperatures above the economizer exit temperatures. Very little of the chlorine in the coal ended up in the ash, from 1.2% to 1.7% of the total chlorine was in the ash. This means that most of the chlorine in the coal would be expected to be in the gas phase at the SCR inlet.

Table 5. Composition of ash collected from ESP silos 3 and 4 (first test series).**Table 5. Ash composition: Major elements as wt% oxides, SO₃-free basis.**

	Coal 3/28/03	Economizer Ash 3/28/03	ESP Ash 3/38/03
SiO ₂	46.7	47.9	47.5
Al ₂ O ₃	19.9	19.5	20.1
TiO ₂	1.4	1.3	1.3
Fe ₂ O ₃	6.4	6.3	5.8
CaO	16.3	16.3	16.6
MgO	4.9	4.9	4.6
K ₂ O	1.1	0.9	1.0
Na ₂ O	1.6	1.3	1.4
P ₂ O ₅	1.0	0.8	1.0
SrO	0.25	0.25	0.27
BaO	0.46	0.44	0.49
MnO	0.03	0.03	0.02

Ash sample	Date	LOI, wt%	Hg, µg/g	Cl, µg/g	% Hg in Ash	% Cl in Ash
Economizer	3/28/03	0.08%	0.0053	28.6	0.03%	1.71%
ESP, silos 3&4	3/28/03	0.31%	0.0809	20.2	0.41%	1.21%
ESP, silos 3&4	3/31/03	0.37%	0.118	24.6	--	--
ESP, silos 3&4	4/1/03	0.31%	0.127	23.6	0.44%	1.20%
ESP, silos 3&4	4/2/03	0.34%	0.101	26.8	0.55%	1.11%

The composition of the flue gas can be estimated from the coal composition. Based on the ash composition, we assume that all of the chlorine in the coal is present as HCl. NO_x was not measured during the first mercury test period, but just prior to the test period, NO_x was about 400 ppm at full load. Table 6 gives the estimated flue gas composition for the first test series.

Table 6. Flue gas composition estimated from coal composition for first test series, except as noted.

	3/28/03	4/1/03	4/2/03
Excess Air	35%	35%	35%
O ₂	4.0%	4.0%	4.0%
CO ₂	13.3%	13.4%	13.5%
H ₂ O	10.6%	10.2%	10.0%
N ₂	72.0%	72.3%	72.4%
SO ₂ [ppm]	317	292	360
HCl [ppm]	7.5	10.1	12.8
NO _x [ppm]*	400	400	400
Hg, ug/dnm ³ (5%O ₂)	8.02	10.82	8.46

*Estimated from previous measurements

During the second test series, coal samples were obtained at the outlet of Mills 1 and 2, and Mills 6 and 7. The samples were composited and analyzed. The results are presented in Table 7. The coal blend was the same as in the first test series, nominally 87% PRB subbituminous and 13% eastern bituminous. The heating value of the coal was commensurate with the blend, as was the coal chlorine content. The mercury content of the coal was equivalent to 4-6 µg/nm³ of mercury, if all the mercury were in the flue gas at 5% O₂.

The ash composition of the coal was not measured for the second test series. The heating value, sulfur and ash contents of the August coal samples were consistent with the March coal samples on a dry basis. However, the average moisture content of the August coal samples was low compared to the moisture content of the March samples: 16% versus 26%. The mercury content was also lower in the August samples on a dry basis.

It is likely that the hot air introduced into the pulverizer drove off some of the mercury and moisture from the coal into the combustion air. This could account for the apparent decrease in coal mercury (and moisture content) as compared to the first test series. The Ontario Hydro results, discussed below, substantiate this conclusion. The effect of temperature on loss of mercury from Powder River Basin (PRB) subbituminous coals is illustrated in Figure 4. At thermal treatment temperatures above 300°F, a substantial amount of the mercury can be lost from PRB coals. Contrasting the March coal samples with the August coal samples (Figure 5), suggests that as much as 45% of the mercury in the coal was driven into the combustion gas in the pulverizers.

Date	8/7/2003	8/8/2003	8/10/2003	8/11/2003	8/12/2003	8/13/2003	8/15/2003	8/16/2003
(As Received):								
Carbon	60.79	60.75	61.31	60.77	61.57	61.62	61.70	61.36
Hydrogen	3.87	4.11	4.16	4.03	4.02	3.74	3.16	3.25
Oxygen	12.27	11.32	11.96	11.29	11.47	12.00	12.79	13.30
Nitrogen	0.86	0.93	0.90	0.91	0.92	0.90	0.85	0.88
Sulfur	0.35	0.38	0.38	0.37	0.40	0.40	0.40	0.39
Ash	5.71	6.17	6.14	6.02	6.07	6.05	6.56	6.23
Moisture	16.15	16.34	15.15	16.61	15.55	15.30	14.53	14.60
HHV , Btu/lb	10,337	10,120	10,395	10,314	10,346	10,418	10,404	10,471
(Dry Basis):								
Hg, ug/g	0.062	0.045	0.049	0.050	0.046	0.048	0.055	0.049
Cl, ug/g	104.0	97.4	125.0	110.0	101.0	244.0	241.0	166.0
SO ₂ , lb/MBtu	0.68	0.74	0.73	0.71	0.77	0.76	0.77	0.75
Hg, lb/TBtu	5.04	3.74	3.99	4.01	3.78	3.91	4.51	4.01
Hg, ug/dnm ³ (5%O ₂)	5.98	4.29	4.67	4.70	4.40	4.64	5.48	4.93

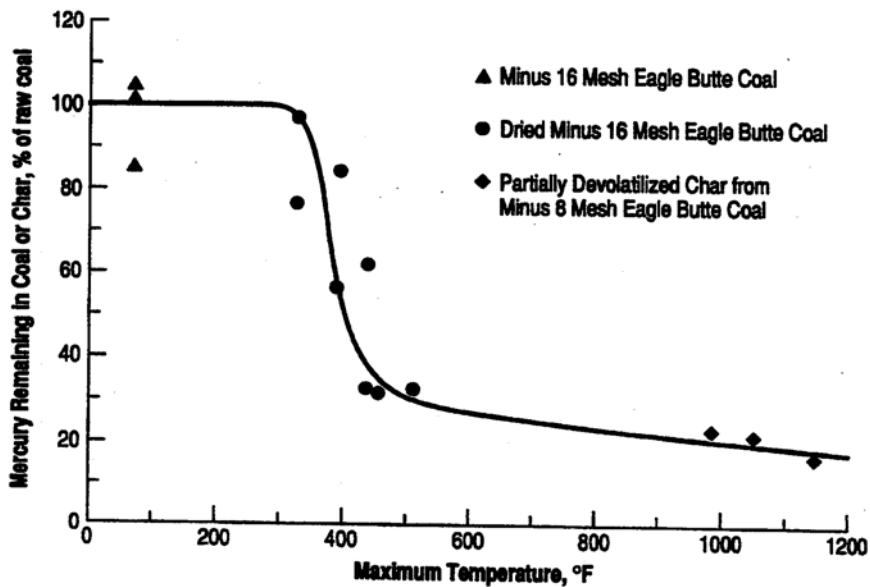


Figure 4. Mercury remaining in Eagle Butte subbituminous coal after thermal treatment. (Source: Reference 13)

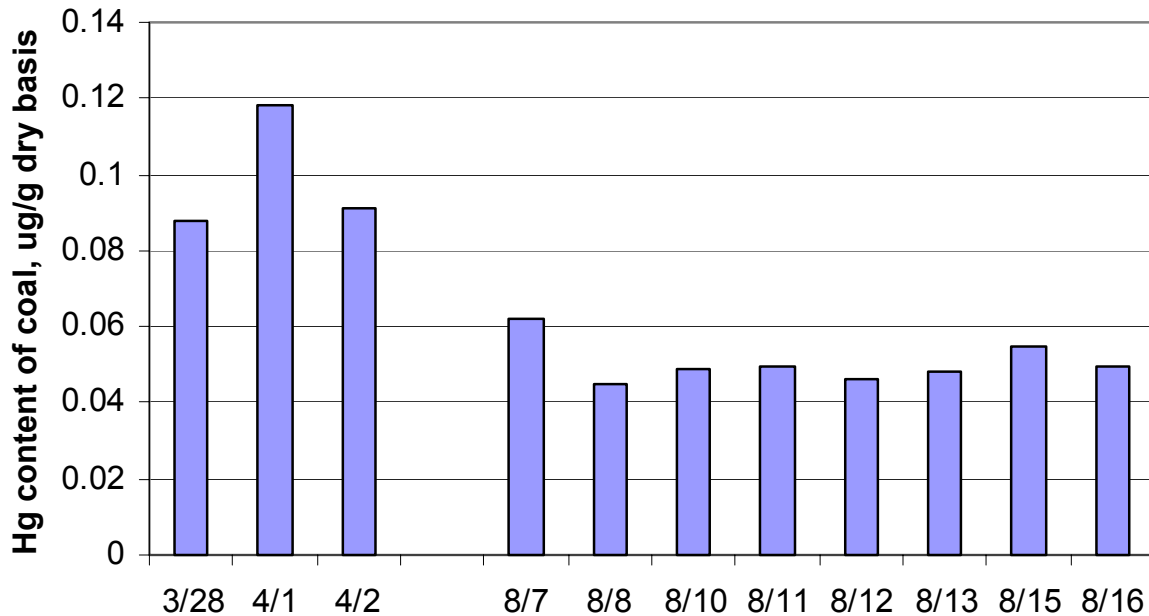


Figure 5. Coal mercury content as a function of sample date.

Ash samples from the second test series were collected from ESP hoppers and analyzed for LOI, Hg and Cl, as shown in Table 8. The LOI of these samples was generally low. Since the ash was a pale tan color, the carbon content of the ash is probably even lower than indicated by the LOI values. In any case, the ash had a very low amount of unburned carbon. The ESP ash had 10 to 100 times more mercury than the economizer ash sample; this suggests that there was some adsorption of mercury by the ash that took place between the economizer and the ESP (probably post-air preheater). However, the amount of mercury adsorbed on the ESP ash was less than 0.5% of the mercury in the coal, based on the g Hg/g of coal. Thus, the fly ash from Rockport was unreactive toward mercury. Mercury levels in the ash from the August samples were comparable to the March/April samples.

Table 8. Composition of ash collected from ESP hoppers (second test series).

Description	MTI ID	Sampled	LOI, wt%	Hg, $\mu\text{g/g}$	% Hg in Ash	Cl, $\mu\text{g/g}$	% Cl in Ash
Economizer Ash	03-245	8/11/2003	0.00	0.0050	0.045%	<5	<0.3%
Economizer Ash	03-246	8/15/2003	0.00	0.0004	0.003%	<5	<0.2%
Fly Ash 3+4	03-242	8/7/2003	0.06	0.0337	0.23%	21	1.38%
Fly Ash 3+4	03-243	8/11/2003	0.30	0.0502	0.45%	21	0.67%
Fly Ash 3+4	03-244	8/15/2003	0.13	0.0549	0.47%	23	1.01%

In contrast to the March/April samples, the chlorine content of the fly ash from the ESP was higher than that from the economizer ash. The chlorine content of the fly ash was similar to that for the March/April tests. Very little of the chlorine in the coal appeared to have ended up in the fly ash, from 0.7% to 1.4% of the total chlorine was in the fly ash in the ESP, based on g Cl/g coal. The low levels of chlorine in the economizer ash suggest that the chlorine should be in the gas phase upstream of the air preheater.

The composition of the flue gas can be estimated from the coal composition. Based on the ash composition, we assume that all of the chlorine in the coal is present as HCl. NO_x averaged about 330 ppm (wet basis, 5% O₂) during the tests. Table 9 gives the estimated flue gas composition. Since it seems likely that moisture was lost in the pulverizer, the concentrations have been adjusted to a coal moisture content of 26.5%, which was the moisture content of the March coal samples.

Table 9. Flue gas composition estimated from coal composition for second test series, except as noted; coal moisture content adjusted to 26.5%.

	8/7/2003	8/8/2003	8/10/2003	8/11/2003	8/12/2003	8/13/2003	8/15/2003	8/16/2003
O ₂	5.0%	5.0%	5.0%	5.0%	5.0%	5.0%	5.0%	5.0%
CO ₂	12.8%	12.6%	12.6%	12.6%	12.7%	12.9%	13.3%	13.2%
H ₂ O	9.1%	9.3%	9.3%	9.2%	9.2%	8.9%	8.5%	8.6%
N ₂	73.0%	73.0%	72.9%	73.0%	73.0%	73.1%	73.1%	73.0%
SO ₂ [ppm]	278	293	295	286	307	312	324	318
HCl [ppm]	6.1	5.6	7.3	6.4	5.9	14.4	14.8	10.2
NO _x [ppm]*	330	330	330	330	330	330	330	330
Hg, ug/dnm ³ (5%O ₂)	5.94	4.26	4.64	4.67	4.37	4.60	5.44	4.89

*Estimated from previous measurements

Gas-phase halide measurements were made on August 8 and the results are given in Table 10. Three runs were made but the results of the second run were not valid. The relatively low chlorine content of the ash samples suggested that most of the chlorine would be found in the gas phase before the air preheater. The low levels of chloride measured in the gas phase were puzzling. It is possible that gaseous chlorine compounds adsorbed on the ash within the sampling system. It would have been better to take the gas sample for the halide measurements at the port used for the Ontario Hydro measurements in order to determine with more certainty if the chlorine compounds were in the gas phase at the inlet to the slipstream reactor.

Table 10. Results of halide measurements in gas, corrected to 5% O₂ (wet basis).

	Chloride, ppm	Cl ₂ , ppm	Fluoride, ppm	F ₂ , ppm
Run 1	0.57	<0.030	0.94	<0.000
Run 3	0.25	<0.042	0.41	<0.001
Average	0.41	<0.036	0.67	<0.001

NO_x Performance

NO_x data were also obtained in late March and early April (approximately 300 hours of operating time on flue gas) and in late August at the conclusion of the second mercury sampling campaign (approximately 2200 hours of operating time on flue gas). These data were analyzed to look at the effects of operating conditions and catalyst age on NO_x reduction. These data have also been reported under REI's NO_x control program (cooperative agreement DE-FC26-00NT40753); analysis of the data was carried out jointly between the two programs.

Appendix B contains the NO_x data from the blank catalyst as well as catalysts C2 through C6. The NO_x concentration at the inlet is calculated at 5% O₂. The inlet concentration has been interpolated based on measurements of the inlet concentration made before and after the measurement of the NO_x concentration at the outlet of each chamber. The ammonia concentration was calculated at 5% O₂, based on the total flow measured in the slipstream reactor and the set point of the ammonia mass flow controller. The NH₃/NO ratio is calculated from the ammonia concentration divided by the estimated inlet NO_x concentration. The average catalyst chamber temperature is calculated from the average of the temperature before the catalyst and at the exit of the catalyst chamber. The space velocity is calculated at 32°F (0°C).

There were differences in the temperatures, space velocities and ratios of NH₃/NO between the March/April data and the August data. In order to compare the NO_x reduction, the effects of these parameters must first be characterized.

The March/April data were taken at excess ammonia (NH₃/NO ~ 1.2-1.6) in order to remove any effects of ammonia concentration. The catalyst temperatures were in the range of 620-650°F. The main factor that affected the NO_x reduction was the space velocity. Figure 6 shows the NO_x reduction as a function of space velocity for all five catalysts. The NO_x reduction for catalysts C2, C3 and C4 appeared to follow a single curve with space velocity. Catalysts C5 and C6 had different levels of NO_x reduction from the other three; the slopes were about the same, but the intercepts were different.

Some of the August NO_x data were taken during the mercury testing; at this time the ammonia to NO ratio was varied. As the NH₃/NO ratio dropped below 0.95, the NO_x conversion began to fall off. This is seen in Figure 7, which shows the NO_x reduction as a function of NH₃/NO ratio at fixed temperatures and space velocities.

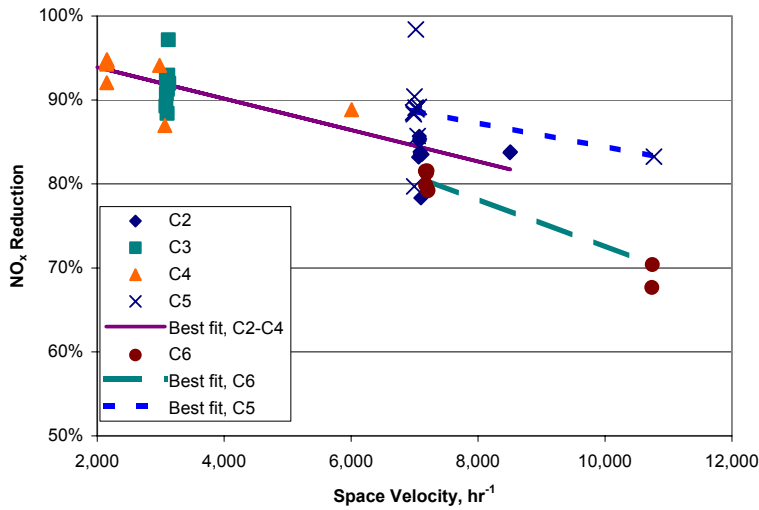


Figure 6. NO_x reduction as a function of space velocity for commercial catalysts from March/April for excess ammonia and catalyst temperatures in the range of 620-650°F.

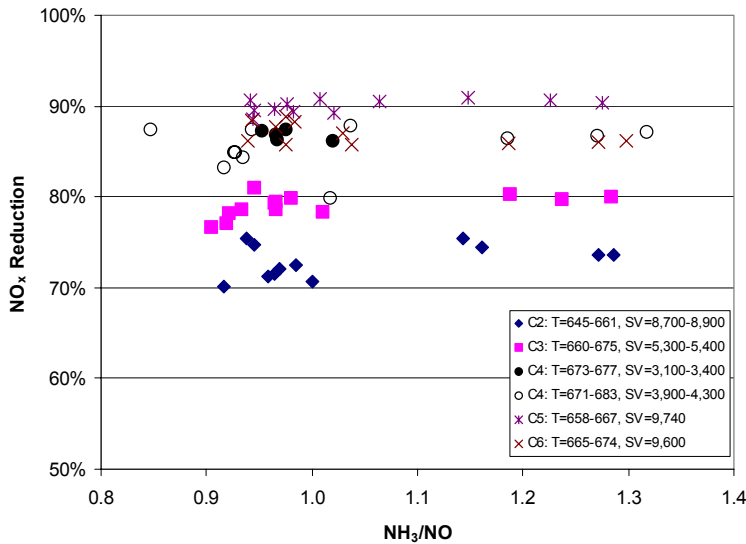


Figure 7. NO_x reduction as a function of NH₃/NO ratio for commercial catalysts from August; temperatures (in degrees F) and space velocities (in hr⁻¹) as indicated on legend.

The effect of temperature on NO_x reduction can also be seen in the August data. Figure 8 shows the NO_x reduction as a function of temperature at a fixed space velocity, all for NH₃/NO > 0.95. Since the March/April data were obtained at different temperatures and space velocities than the August data, the August data were corrected for temperature by using the curvefits shown in Figure 8 and Table 11. Such curvefits should not be used for large temperature corrections; however, the upper end of the range of temperatures in March/April data is generally close (0 to 8°F) to the lower end of the August temperature range for catalysts C2 through C5. There is a 20°F gap in temperature ranges for C6; therefore extrapolation of the C6 data is suspect.

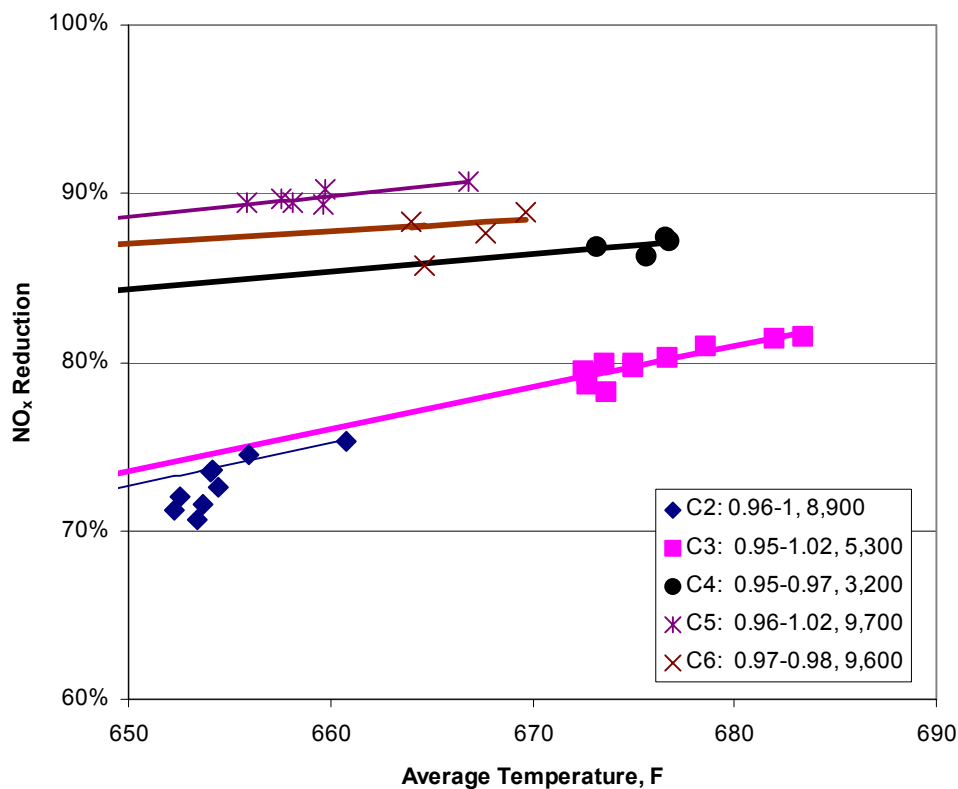


Figure 8. NO_x reduction as a function of temperature for commercial catalysts from August; NH₃/NO ratios and space velocities (in hr⁻¹) as indicated on legend.

Table 11. Relationship between NO_x reduction and temperature from August test data.

Catalyst	C2	C3	C4	C5	C6
Space velocity, hr ⁻¹	8,900	5,300	3,200	9,700	9,600
NH ₃ /NO	1.14-1.29	0.95-1.02	0.97-0.97	0.96-1.02	0.97-0.98
Temperature range, °F	653-661	674-683	676-685	660-669	670-675
r ²	0.95	0.80	0.38	0.68	0.12
Intercept	-97.2	-87.1	16.7	9.2	39.4
Slope	0.261	0.247	0.104	0.122	0.073

Figure 9 compares the March/April NO_x data with the August NO_x data. The August data show the range of NO_x reductions that correspond to the temperature range of the data of the March/April data. Catalysts C2, C3 and C4 appear to have lower NO_x reduction in August as compared to March/April. Catalyst C5 has about the same NO_x reduction. Catalyst C6 appears to have higher NO_x reduction in August as compared to March/April; however, extrapolating the C6 NO_x reduction to the range of temperatures of the March/April tests may produce larger errors than for the other catalysts, as discussed previously.

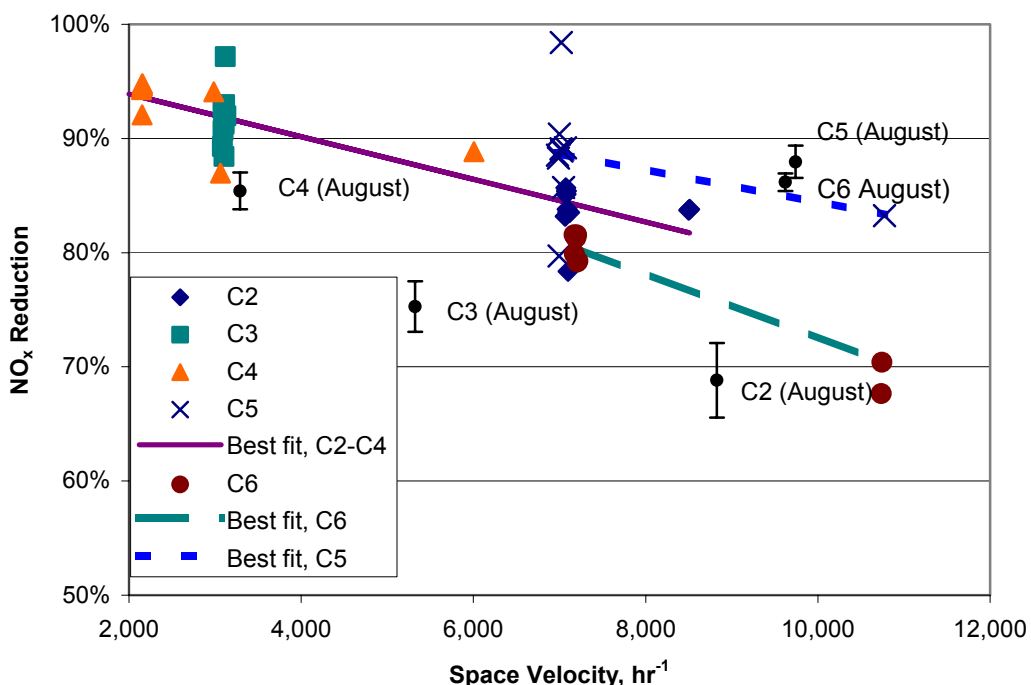


Figure 9. NO_x reduction as a function of space velocity for commercial catalysts from March/April for excess ammonia and catalyst temperatures in the range of 620-650°F compared with August data (extrapolated to the appropriate temperature range).

Mercury Speciation Data

During the first test series, Ontario Hydro measurements were made on March 28, 2003. Table 12 summarizes the three Ontario Hydro measurements, with an average value. The amount of particulate mercury was very low, about 1.7% of the total mercury measured. The ESP ash had about 0.4% of the total mercury, based on the coal composition. Both of these measurements suggest that the fly ash does not adsorb any significant amount of mercury. Figure 10 compares the average Ontario Hydro total mercury with the total gaseous mercury (averaged from the test period) from the SCEM and the total mercury based on the coal composition, all corrected to 5% O_2 . There was good agreement between the total mercury measurement by SCEM, Ontario Hydro and coal composition.

Table 12. Ontario Hydro measurements for first test series (28 March 2003); mercury concentrations in $\mu\text{g}/\text{Nm}^3$ at 5% O_2 .

Gas Vol. Sampled	Gas Vol. Sampled	Oxidized Hg	Elemental Hg	Total Hg	Oxidized Hg	Elemental Hg	Particulate	Total Hg
(dscf)	(Liters -dry)	(μg)	(μg)	(μg)	($\mu\text{g}/\text{Nm}^3$)	($\mu\text{g}/\text{Nm}^3$)	($\mu\text{g}/\text{Nm}^3$)	($\mu\text{g}/\text{Nm}^3$)
62.153	1760.71	1.50	11.78	13.28	0.86	6.78	0.12	7.76
62.992	1784.48	1.88	10.03	11.91	1.06	5.69	0.13	6.89
60.351	1709.66	1.97	10.18	12.15	1.17	6.03	0.13	7.33
61.83	1751.61	1.78	10.66	12.45	1.03	6.17	0.13	7.33

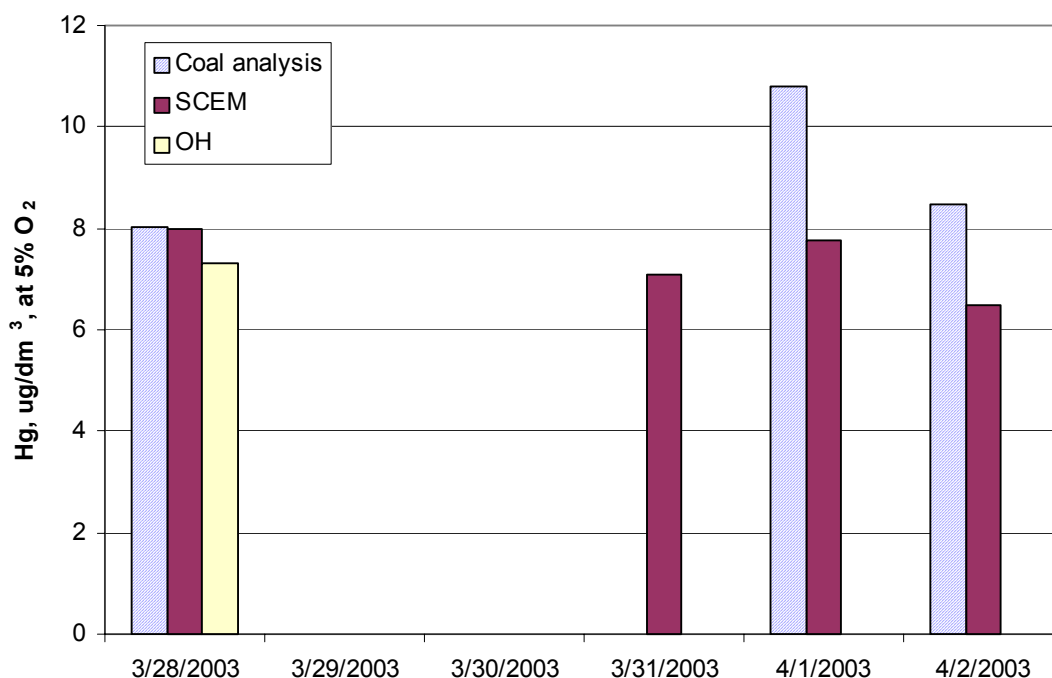


Figure 10. Total mercury measurements, $\mu\text{g}/\text{Nm}^3$ for first test series, corrected to 5% O_2

During the second test series, three Ontario Hydro measurements were made: two on August 7 and one on August 8. The results of the Ontario Hydro measurements are given in Table 13. The Ontario Hydro probe could not be removed from the port immediately after the gas sampling was finished, so the filter was exposed to the flue gas for longer than the gas sampling time (although there was only flow through the filter during the gas sampling period). The amount of mercury on the ash is small. The total ash loading for this coal is estimated to be about $6 \text{ g}/\text{Nm}^3$ at 5% O_2 . This is an upper limit, because the full ash loading may not be drawn into the slipstream reactor. Using $6 \text{ g}/\text{Nm}^3$ and the measured concentration of Hg in the fly ash, the maximum particulate mercury is estimated to be $0.12 \mu\text{g}/\text{Nm}^3$. This would amount to about 1% of the measured gas-phase mercury. This is similar to the measured particulate-phase mercury in

the first test series. This, the amount of particulate-bound mercury will not be reported; however, it is probably only about 1% of the total mercury at the sampling location.

Table 13. Ontario Hydro measurements for second test series, corrected to 5% O₂.

Sample ID	Date of Run	Start Time	Oxidized Hg	Elemental Hg	Total Hg	Fly Ash Hg [*]	Filter Hg
			($\mu\text{g}/\text{Nm}^3$)	($\mu\text{g}/\text{Nm}^3$)	($\mu\text{g}/\text{Nm}^3$)	($\mu\text{g}/\text{g}$)	(μg)
Run 1	7-Aug-03	14:06	0.84	7.75	8.60	0.012	<0.006
Run 2	7-Aug-03	18:18	1.14	7.96	9.10	0.034	0.011
Run 3	8-Aug-03	8:21	1.22	7.62	8.83	0.016	<0.006
Average	-	-	1.07	7.77	8.84	0.0207	

* Fly ash sample taken from filter

Carbon trap samples were also taken. These were not taken at the Ontario Hydro port, but at the location where the SCEM samples were taken. Table 14 summarizes all the “inlet” mercury samples:

- Ontario Hydro samples taken near the reactor inlet
- SCEM measurements taken through the sampling system
- Carbon trap samples taken through the sampling system

The Ontario Hydro measurements made on August 7 agree well with the SCEM measurements for total mercury, although the SCEM measured lower values of elemental mercury than the Ontario Hydro. The Ontario Hydro measurements for total mercury were higher than the equivalent coal mercury. As discussed above, this may be due to vaporization of mercury from the coal in the mill. Any mercury that leaves the coal in the mill will end up in the flue gas, but it would not be measured in the solid samples at the outlet of the mill.

After August 8, the configuration of the sampling system was changed to bypass the heated switching valve and use the URS inertial separation probe. SCEM and carbon trap measurements of inlet mercury made after the change in configuration are lower than the SCEM and Ontario Hydro measurements made on August 7 and 8. This may indicate that there was some loss of mercury in the inertial separation probe.

Table 14. Inlet Mercury concentrations measured by various methods in second test series.

Date	Start	SCEM Measurements				Ontario Hydro		Carbon Trap	Speciation: %Hg ⁰	
		Hg _T	St.Dev	Hg ⁰	St.Dev	Hg _T	Hg ⁰	Hg _T	SCEM	OH
8/7	14:06					8.60	7.75			90%
8/7	14:55	7.07	1.33							
8/7	18:18					9.10	7.96			87%
8/7	18:40	9.83	1.54							
8/7	19:24	9.34	2.27						59%	
8/7	20:36			5.50	1.44					
8/8	8:21					8.83	7.62			86%
8/8	8:46	6.51	0.37							
8/8	10:31	4.89	1.38							
8/11	12:39	5.89	0.43							
8/11	20:03	6.33	0.39							
8/12	10:30							3.54		
8/12	13:27			4.19	0.06					
8/12	13:54	6.26	0.41						67%	
8/12	17:15			4.11	0.32					
8/12	21:04			4.32	0.43					
8/12	21:48	4.25	0.41						99%	
8/13	10:51	5.89	0.32						85%	
8/13	11:18			5.04	0.41					
8/13	14:06			4.90	0.46					
8/13	14:30	4.84	0.39						101%	
8/13	17:38			4.94	0.48					
8/13	18:15	4.99	0.54						99%	
8/15	12:07	5.05	0.33						65%	
8/15	12:39			3.29	0.33					
8/15	20:27			5.96	0.78					
8/15	21:24	6.29	0.38						95%	
8/15	22:14			6.54	0.58					
8/16	10:33	5.24	0.25							
8/16	11:57							5.22		
8/16	12:46			3.73	0.58					

The Ontario Hydro measurements for the second test series corresponded to 88% of gaseous mercury as elemental; the Ontario Hydro measurements for the first test series gave 81% of the gaseous mercury as elemental. The SCEM values for elemental mercury also showed a very high percentage of mercury as elemental. This is in keeping with the moderate to low chlorine levels in the coal and the high calcium in the ash.

Mercury speciation data were obtained for a wide range of space velocities, from 1,000 to 10,000 hr^{-1} . At a single space velocity, data were obtained with and without ammonia. The SCEM data consist of multiple measurements (of either elemental or total mercury). The sample period was twenty minutes for most of the test period. Figure 10 shows one test series, with individual data points.

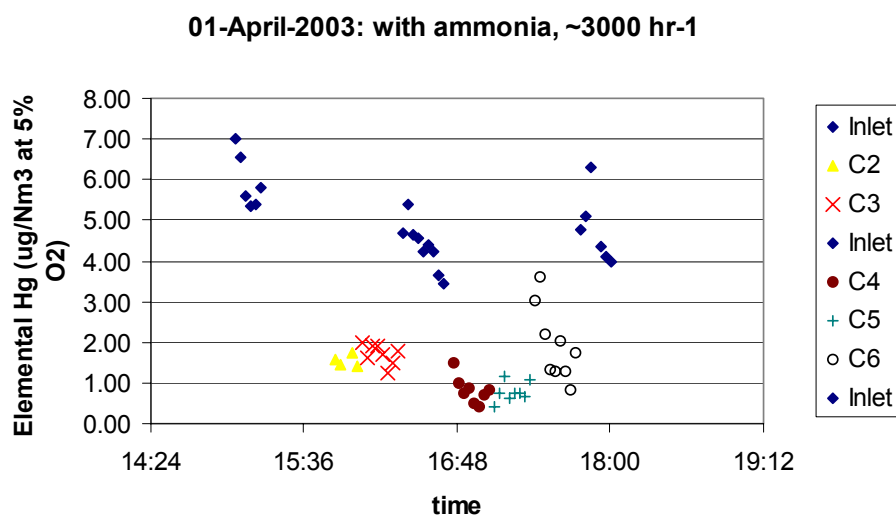


Figure 11. Mercury SCEM data ($\mu\text{g}/\text{Nm}^3$ at 5% O_2) for elemental mercury at 3000-7000 hr^{-1} space velocity with $\text{NH}_3/\text{NO}=5$.

In some cases, the initial points for a given sample location were not used to compute the average value. The average values and the standard deviation (of the data points used) are shown in Figure 12. Appendix C contains the complete set of measurements (average values) for all the tests. The standard deviation of the individual measurements taken at a given data point was reasonable. The average inlet concentration of elemental mercury (or total mercury) appeared stable, when inlet measurements were repeated over a period of several hours. There were some problems with excessive pressure in the catalyst chamber and sample lines due to ash blockage. This resulted in leaks in the sample line and, occasionally, unstable mercury readings.

From the SCEM data on mercury at the inlet and outlet of the chambers, the loss of total mercury across the chamber and the loss of elemental mercury across the chamber were calculated. The inlet value (either Hg^0 or total Hg_T) was measured periodically when the chamber outlet values were being measured (see Figure 11 for an example). In general, the inlet value was fairly constant during a measuring period. In order to calculate the loss of elemental or total mercury across individual chambers, the inlet value was interpolated at the appropriate time.

Figure 13 shows that some loss of total mercury was observed across the commercial catalysts,

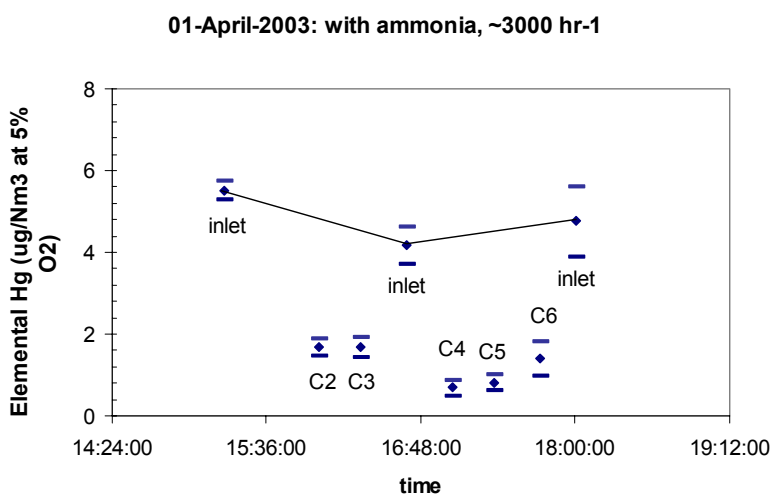


Figure 12. Average values of mercury SCEM data ($\mu\text{g}/\text{Nm}^3$ at 5% O_2) for elemental mercury at 3000-7000 hr^{-1} space velocity with $\text{NH}_3/\text{NO}=5$.

but not across the blank monolith. The values shown in the figure were calculated from average values of inlet and outlet mercury. The error bars on the figure were computed from the standard deviation of the average measured values using a quadratic formula. Note that errors in the measurement itself have not been included.

There was no loss of total mercury across the blank monolith, but there was loss of mercury across the commercial catalysts. It is

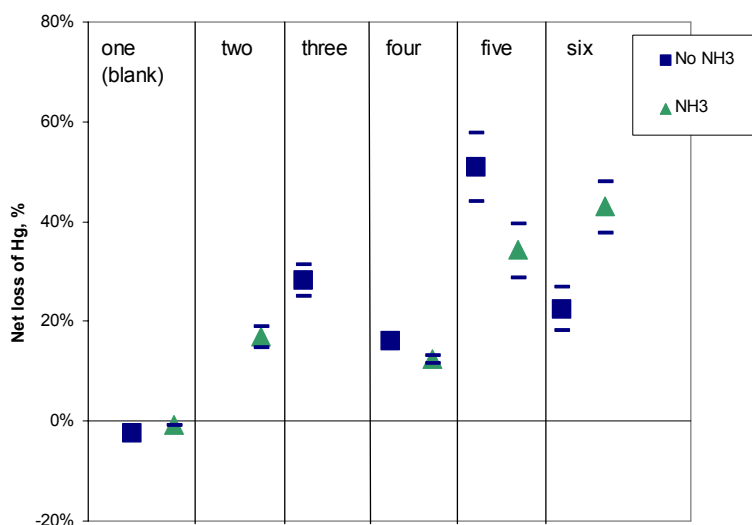


Figure 13. Calculated loss of total mercury across for the first test series catalyst chambers for space velocity of 2,000-5,000 hr^{-1} , with and without ammonia ($\text{NH}_3/\text{NO}=2.4$).

important to note that the inlet sample line is approximately three times longer than the outlet sample lines; all are heated stainless steel. There are Teflon lines inside the heated switching valve assembly. If there were a significant loss of mercury in the samples lines, there would be less mercury measured from the inlet line as compared to the outlet line from the blank monolith. That was not observed.

There are several possible explanations for the observed loss of mercury on the commercial catalysts and the absence of such loss across the blank monolith. There could be adsorption of mercury by the commercial catalysts. This has been observed by URS and others on fresh catalyst. In the first test series, the catalysts had been exposed to flue gas in total for only 200-300 hours. Furthermore, the catalysts were off-line for cleaning right before the mercury testing began. Thus, if there were a transient adsorption of mercury, it might have been more pronounced at the start of the testing. In Figure 14, the loss of total mercury across the catalysts is plotted as a function of time from the start of flue gas flow; this graph starts at zero, corresponding to the time when the slipstream reactor was brought back on line after cleaning. There is no clear effect of time in the range of 0 to 80 hours.

One of the problems that could occur in the sampling system is preferential loss of oxidized mercury. Elemental mercury is expected to be less reactive with surfaces in the sampling system than oxidized mercury. If oxidized mercury were preferentially being removed in the sampling system, one would expect to see larger losses of total mercury as the amount of oxidized mercury at the outlet of the reactor increased (or the amount of elemental mercury decreased). Instead, the opposite trend was observed in Figure 15: the loss of mercury across the commercial catalysts was greatest when there was more elemental mercury leaving the catalyst. Note that this was not true for the blank monolith, which had a lot of elemental mercury leaving the catalyst but no loss of total mercury across the catalyst.

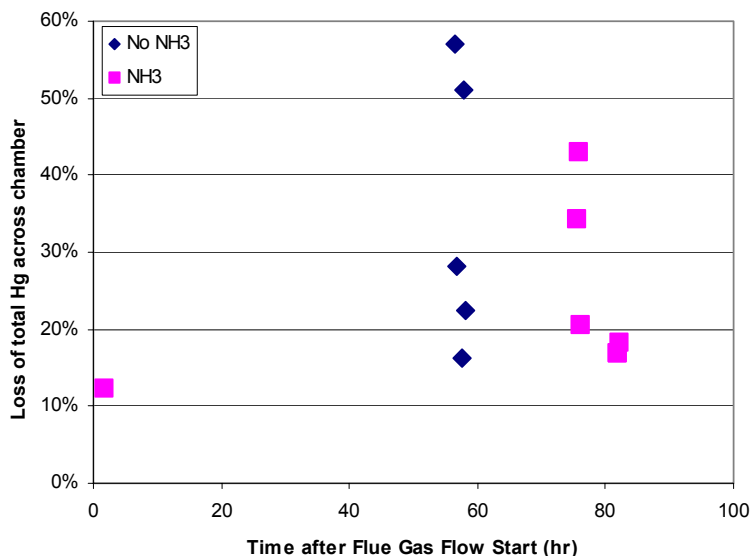


Figure 14. Loss of total mercury across commercial catalysts as a function of time since last start-up of reactor for the first test series.

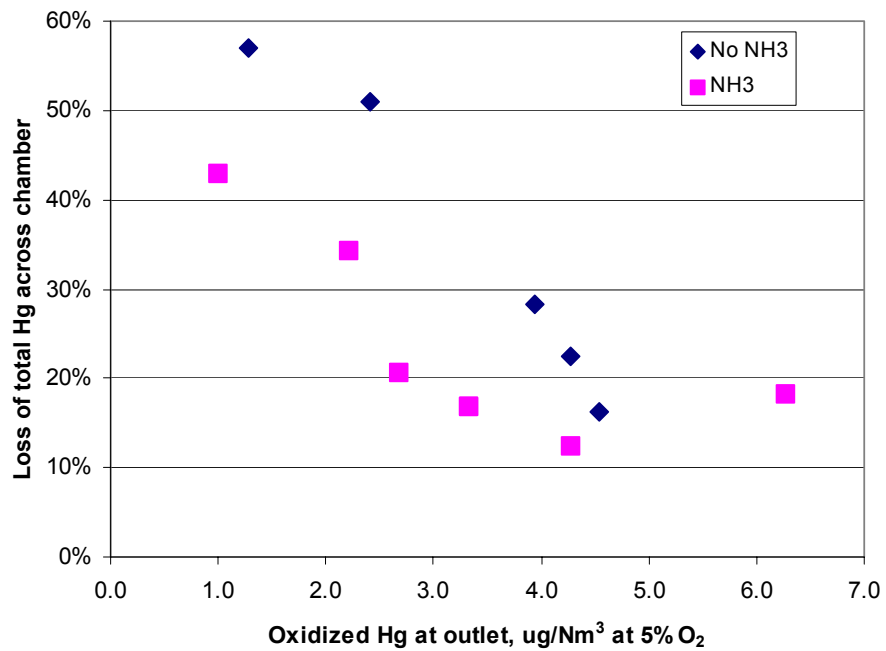


Figure 15. Loss of total mercury across commercial catalysts for the first test series as a function of oxidized mercury at outlet (estimated from separate elemental mercury measurements).

catalysts did not. At typical space velocities for full-scale SCR catalysts, the oxidation was 60 to 80%.

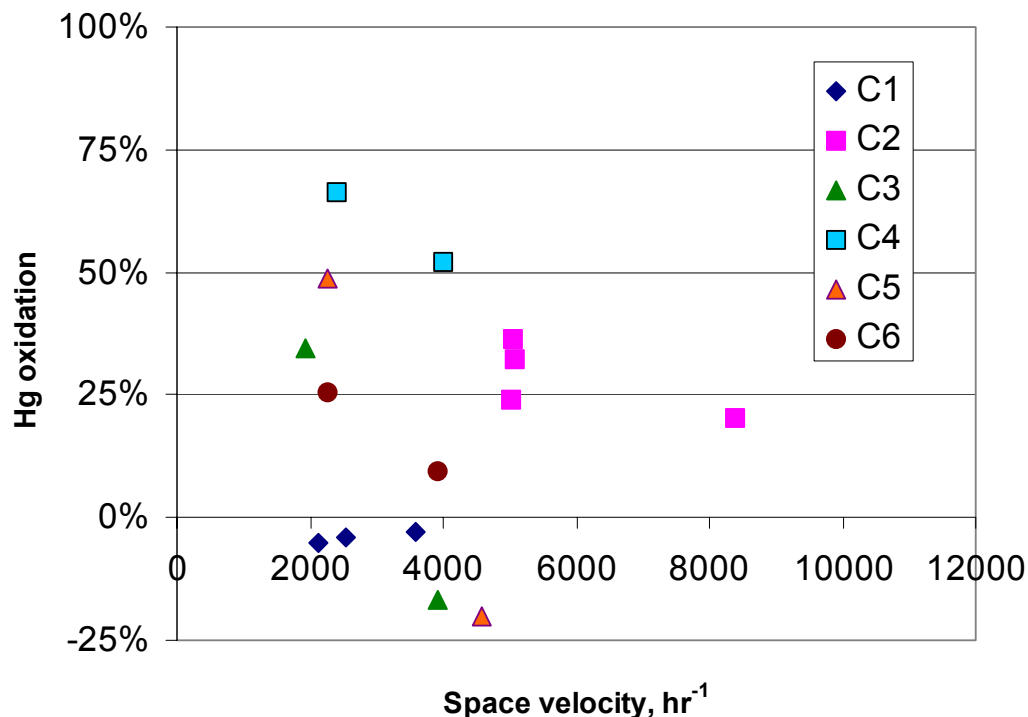


Figure 17. Oxidation (net loss of elemental mercury) in the first test series at 650°F as a function of space velocity for excess ammonia (NH₃/NO: 1.2-2.0).

The presence of ammonia inhibited oxidation of mercury in some cases. Figure 18 compares oxidation with and without ammonia. Catalyst C1 (blank monolith) does not show any mercury oxidation, with or without ammonia present. Catalysts C3 and C6 (plate and monolith, respectively) clearly show an effect of ammonia. Catalysts C4 and C5 (plate and monolith, respectively) appear to show an effect of ammonia, although the values are close, given the uncertainty in the data. The amount of oxidation without ammonia was about the same for all the catalysts (60 to 80%), but when ammonia was present, there was a much larger range of mercury oxidation values.

Preliminary results show that the blank catalyst did not oxidize mercury (with or without ammonia). Furthermore, the concentration of total mercury at the inlet and outlet of the blank catalyst agreed well.

Data from the exit of the commercial catalysts shows a pronounced effect of space velocity on mercury oxidation across the catalysts for most of the commercial catalysts. As has been observed by others, mercury oxidation tends to fall off at high space velocities. The commercial catalysts appeared to remove mercury, based on total mercury measurements. The amount of mercury oxidized across the commercial catalysts increased when there was not ammonia in the flue gas.

Owing to various equipment problems during the sampling period, certain planned measurements did not take place during the test period, specifically the measurement of chlorine

in the flue gas and the carbon trap measurements of total mercury. These will be done during the second test series.

Measurements of elemental mercury were made in the second test series on August 12 and 13 in order to examine the loss of elemental mercury (oxidation) across the catalysts. Figure 19 shows the SCEM data for those days. The inlet concentration of elemental mercury was consistent across multiple samples. On August 12 the concentration of elemental mercury at the outlet of the blank chamber (C1) was higher than the inlet value, although not on August 13.

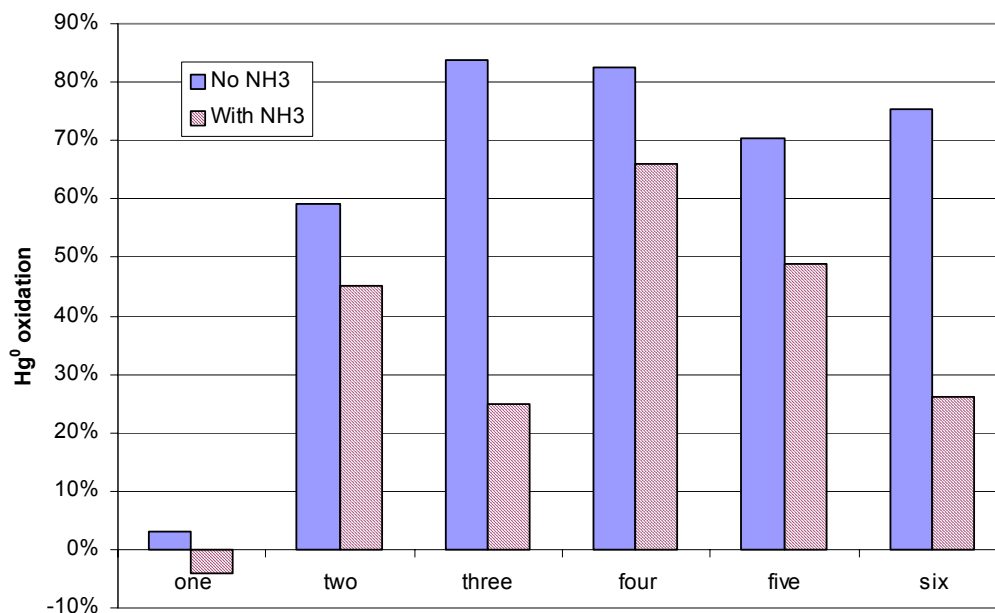


Figure 18. Estimated loss of elemental mercury in the first test series across catalyst chambers for space velocity of $2,500 \text{ hr}^{-1}$, with and without ammonia ($\text{NH}_3/\text{NO}=1.2\text{-}2.0$).

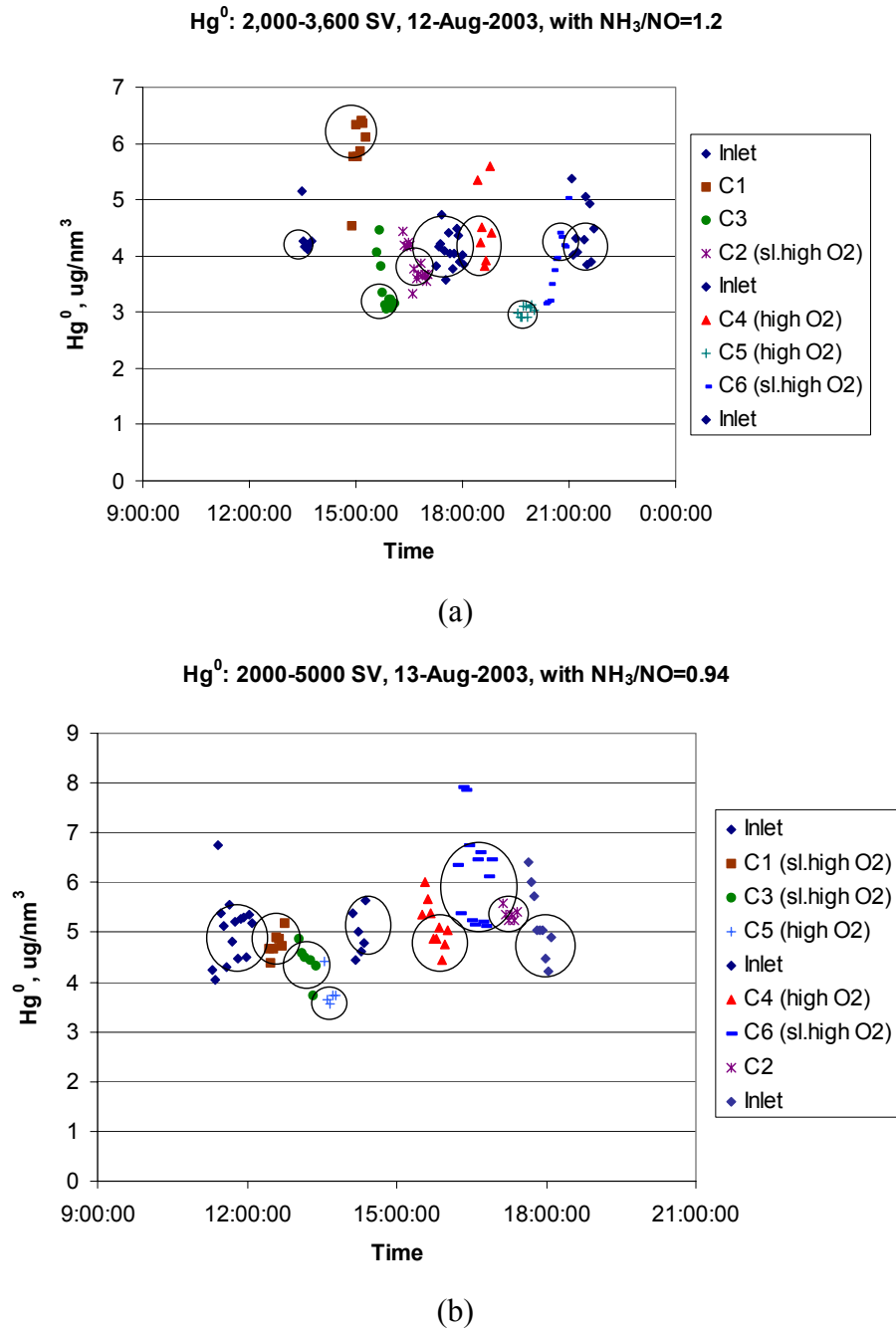


Figure 19. SCEM measurements of elemental mercury during the second test series at SV=2000-5000 hr⁻¹ and NH₃/NO=0.94-1.2: (a) August 12 and (b) August 13.

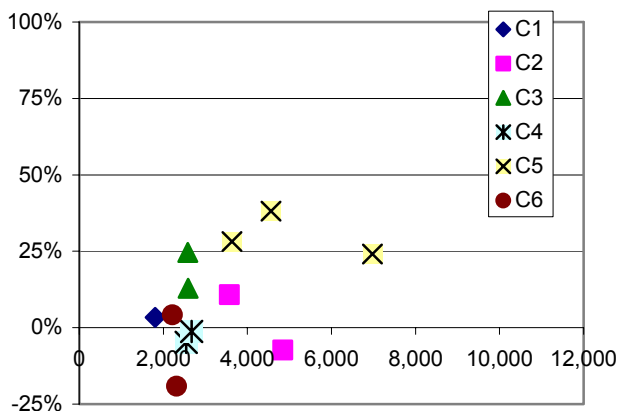


Figure 20. Mercury oxidation as a function of space velocity for $\text{NH}_3/\text{NO} = 0.9-1.2$.

The effect of space velocity on mercury oxidation is shown in Figure 20. The values shown in the figure were calculated from average values of inlet and outlet mercury. The blank monolith (C1) did not show any oxidation of elemental mercury. For the commercial catalysts, oxidation was less than 50% in general with catalysts C4 and C6 showing negligible oxidation. The range of space velocities was lower for the second test series than for the March/April test series. Figure 21 compares the oxidation data from the first test series to that from the second test series. For two of the catalysts (C3 and C5), oxidation during the second test series was comparable to that in the first test series. Catalyst C2 (monolith) showed some oxidation in the second test series, although not as much as in the first test series. Catalysts C4 and C6 showed negligible oxidation in the second test series.

The effect of space velocity on mercury oxidation is shown in Figure 20. The values shown in the figure were calculated from average values of inlet and outlet mercury. The blank monolith (C1) did not show any oxidation of elemental mercury. For the commercial catalysts, oxidation was less than 50% in general with catalysts C4 and C6 showing negligible oxidation. The range of space velocities was lower for the second test series than for the March/April test series. Figure 21 compares the oxidation data from the first test series to that from the second test series. For two of the catalysts (C3 and C5), oxidation during the second test series was comparable to that in the first test series. Catalyst C2 (monolith) showed some oxidation in the second test series, although not as much as in the first test series. Catalysts C4 and C6 showed negligible oxidation in the second test series.

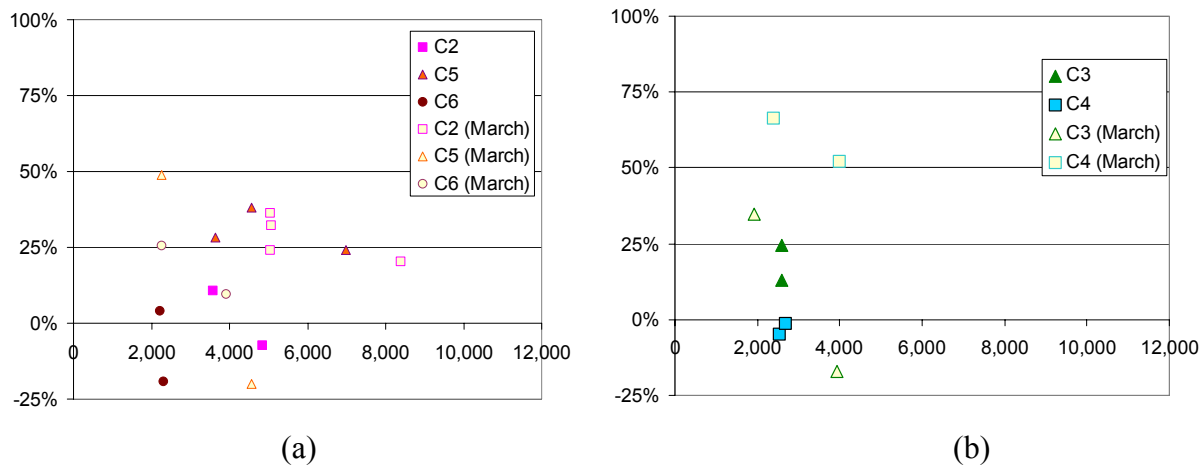


Figure 21. Comparison of mercury oxidation from the first test series ($\text{NH}_3/\text{NO}: 1.2-2.0$) and the second test series ($\text{NH}_3/\text{NO}: 0.9-1.2$) with ammonia: (a) monolith catalysts and (b) plate catalysts.

During the first test series, a decrease in mercury oxidation was noted in the presence of excess ammonia. The data taken on August 15 were without ammonia. However, there was a lot of scatter in the data (Figure 22), so it is hard to interpret the data, particularly as the inlet value of elemental mercury changed from the beginning to the end of the day.

Figure 23 shows the comparison of mercury oxidation with and without ammonia from the first test series and with ammonia

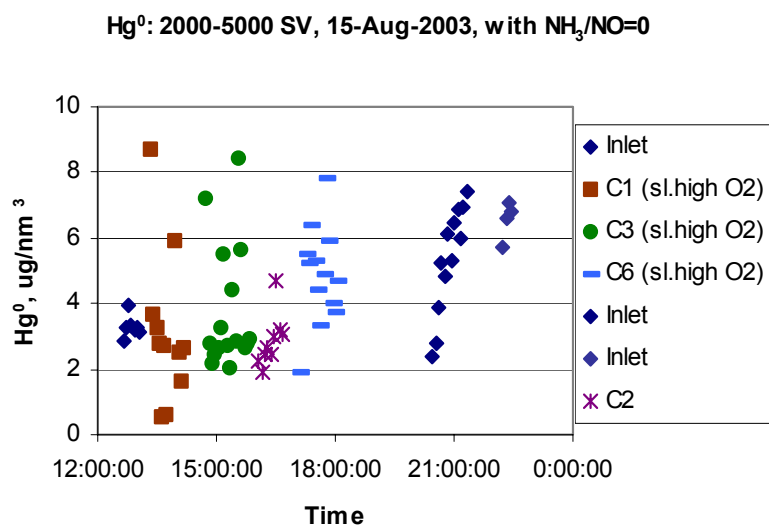


Figure 22. Elemental mercury during second test series, SV=2000-4000 hr⁻¹.

for the second test series. For both test series, graphs of mercury oxidation as a function of space velocity were used to estimate the oxidation at a space velocity of 2,500, using a linear extrapolation or interpolation. Catalysts C3 (plate) and C5 (monolith) showed similar mercury oxidation between the first and second test series. Catalysts C2 and C6 (monolith) and catalyst C4 (plate) showed less oxidation in the second test series as compared to the first test series.

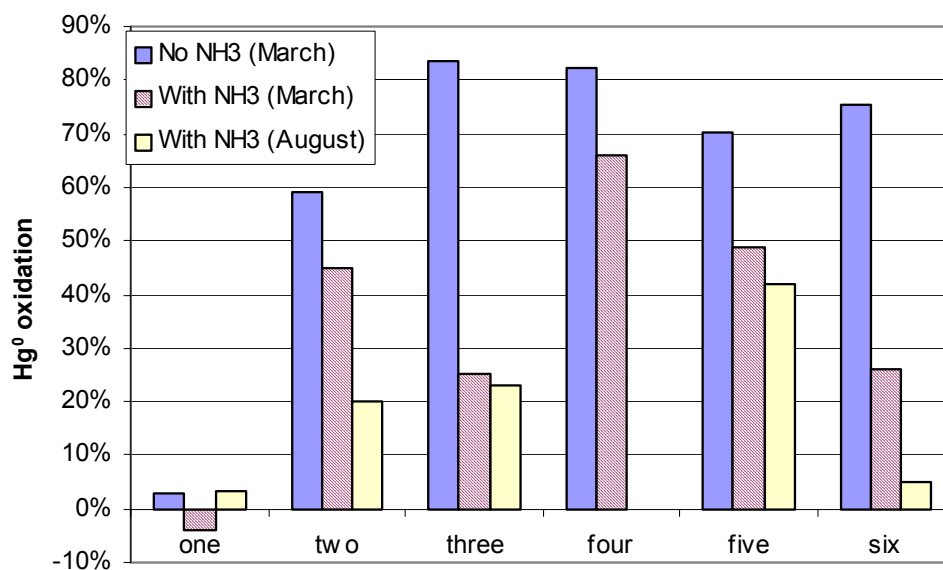


Figure 23. Mercury oxidation with and without ammonia estimate at 2,500 hr⁻¹; March/April test series: NH₃/NO=1.2-2.0; August test series: NH₃/NO=0.9-1.2.

In order to better understand the effects of ammonia on the catalysts, as well as transient behavior, several transient experiments were performed, in which ammonia was turned off or on while mercury and NO_x were measured at the outlet of the catalysts.

Elemental mercury was measured continuously at the exit of catalyst C2 as the ammonia was turned on. Figure 24 shows the concentrations of elemental mercury, NO_x and ammonia as a function of time for this measurement. (The ammonia concentration was calculated from the set point of the ammonia mass flow controller and the total velocity in the slipstream reactor.) The NO_x concentration responds to the ammonia being turned on after 2 to 3 minutes. The time lag is related to both the residence time in the sampling line and the residence time in the ammonia delivery line. It took about ten minutes for the outlet NO_x to reach a constant value. Adding ammonia to the flue gas caused a temporary increase in elemental mercury at the exit of catalyst C2. The large increase in elemental mercury appeared to last about twenty minutes and then the elemental mercury approached some level that was higher than the pre-ammonia level.

However, the measurement had to be terminated because the plant was going to reduce load. The presence of ammonia therefore increased the concentration of elemental mercury at the outlet of C2 from $4 \mu\text{g}/\text{dnm}^3$ to $5 \mu\text{g}/\text{dnm}^3$ —less oxidation took place in the presence of ammonia. Furthermore, mercury seemed to *desorb* from the catalyst when ammonia was added to the flue gas, since the peak concentration of elemental mercury was greater than the measured inlet elemental mercury ($6.54 \mu\text{g}/\text{dnm}^3$).

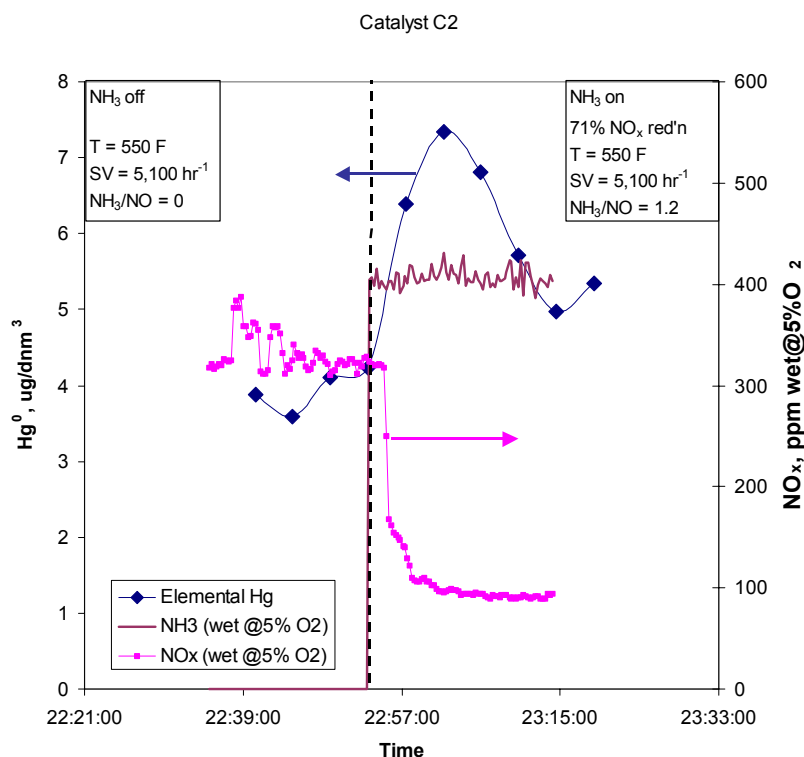


Figure 24. Elemental mercury and NO_x as a function of time for catalyst C2; $T=550^\circ\text{F}$, $\text{SV}=5,100 \text{ hr}^{-1}$.

The transient experiment was repeated with catalyst C5. We also looked at the effect of changing space velocity, as shown in Figure 25. Lowering the space velocity resulted in a decrease in the average temperature in the catalyst chamber, from 600 to 550°F. This may be why the NO_x concentration rose after the space velocity was lowered. The concentration of elemental mercury initially dropped after the space velocity was decreased, but then rose, along with the NO_x concentration. After the ammonia was turned off, the concentration of elemental mercury initially increased, and then dropped. The concentration of elemental mercury before the ammonia was turned off was about $5 \mu\text{g}/\text{dnm}^3$ and after the ammonia was turned off, it dropped to $2 \mu\text{g}/\text{dnm}^3$.

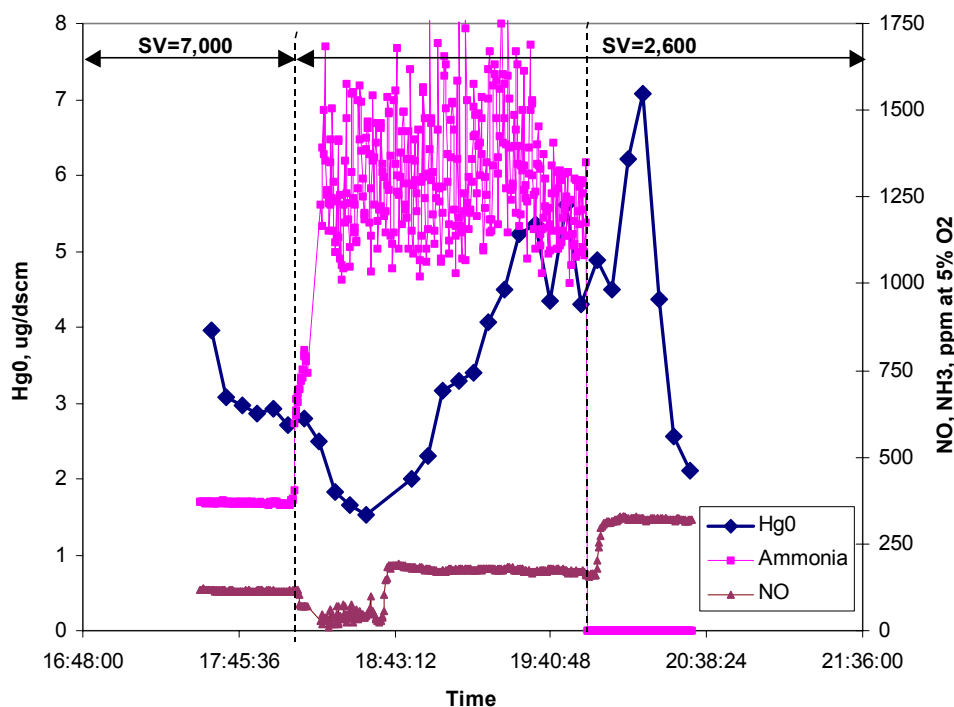


Figure 25. Elemental mercury and NO_x as a function of time for catalyst C5; $T=600^\circ\text{F}$, $\text{SV}=7,000 \text{ hr}^{-1}$, $\text{NH}_3/\text{NO}=1.2$ or $T=540^\circ\text{F}$, $\text{SV}=2,600 \text{ hr}^{-1}$, $\text{NH}_3/\text{NO}=3.75$.

The sampling line for catalyst C5 became blocked, so it was not possible to continue sampling C5. In order to observe the behavior when ammonia was turned on, the exit from catalyst C3 was sampled. Figure 26 shows that when the ammonia was turned on again, the concentration of NO_x returned quickly to the previous level (see Figure 25). The concentration of elemental mercury rose from about $1.8 \mu\text{g}/\text{dnm}^3$ (without ammonia) and peaked after about 45 minutes. The peak concentration of $10.6 \mu\text{g}/\text{dnm}^3$ was far in excess of the observed inlet levels of elemental mercury. Once again, elemental mercury appears to have desorbed from the catalyst when ammonia was turned on. Unfortunately, there was not sufficient time at full load to continue the mercury measurements. It must be noted that the ammonia concentration was very high during the low space velocity experiments because the ammonia was in manual operating mode and was not changed when the flow was changed.

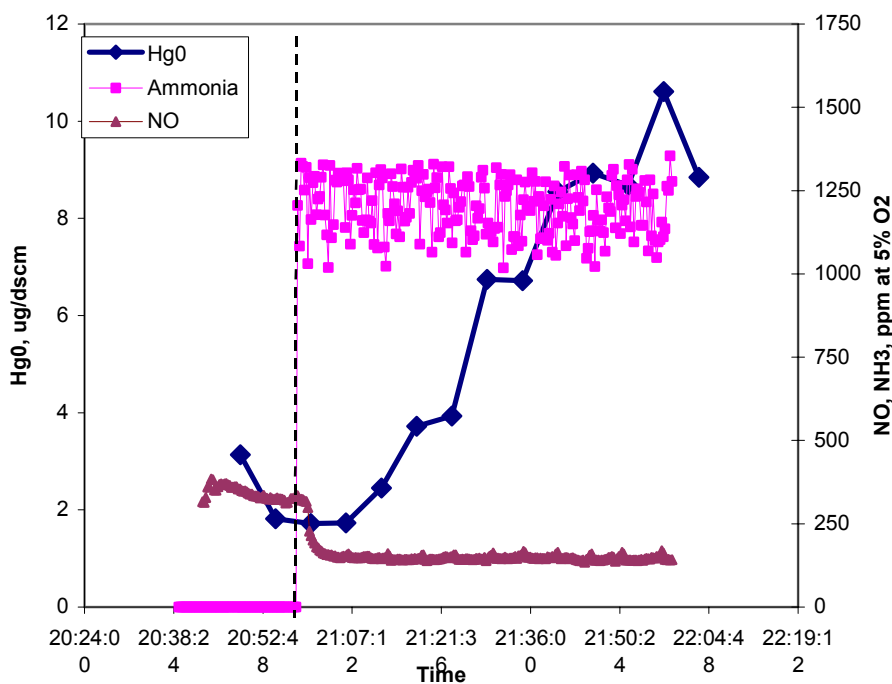


Figure 26. Elemental mercury and NO_x as a function of time for catalyst C3: $T=574$ F. $\text{SV}=1.110 \text{ hr}^{-1}$. $\text{NH}_3/\text{NO}=3.44$.

Task 4 - Data Analysis and Validation

In previous quarterly reports, laboratory, pilot and full-scale data have been reviewed. These data will be summarized briefly here before presenting the rationale for a global mercury oxidation model.

In laboratory work carried out by Hocquel,³ metal oxides were examined individually using synthetic flue gas mixtures to determine if they adsorbed mercury compounds or oxidized elemental mercury. At low levels of HCl in the gas, the metal oxides decreased the amount of HgCl_2 in the gas. This was particularly true for the oxides WO_3 and MoO_3 at SCR temperatures. V_2O_5 significantly increased the amount of HgCl_2 in the gas. Between 130°C and 410°C , the amount of oxidation increased with increasing temperature. No difference in oxidation across V_2O_5 was detected in the absence of oxygen, as compared to with oxygen in the gas. HgCl_2 was not observed to adsorb on SCR catalyst. However, at low HCl concentrations, the amount of HgCl_2 decreased across SCR catalysts, perhaps by reduction of HgCl_2 by MoO_3 or WO_3 .

Elemental mercury was observed to adsorb on commercial SCR catalysts with a capacity on the order a few mg Hg per kg of catalyst.³ The sorption of mercury increased with decreasing HCl concentration. At low HCl concentrations, sorption increased with increasing temperature. A step increase in HCl concentration resulted in release of adsorbed mercury from the catalyst in the form of HgCl_2 . Catalysts with high V_2O_5 content (and similar contents of WO_3 or MoO_3) showed higher adsorption of elemental mercury at a given HCl concentration. SO_2 did not have a strong effect on sorption of elemental mercury.

Elemental mercury was oxidized across commercial SCR catalysts in Hocquel's laboratory study.³ Higher HCl concentration and lower temperatures resulted in higher conversions to HgCl₂. The conclusion of this study was that oxidation of mercury occurred at the active V₂O₅ sites on the catalyst. Hg⁰, HgCl₂ and HCl all compete for the active sites and, of course, compete with NH₃ for those sites.

Lee and coworkers¹ also observed adsorption and oxidation of Hg⁰ to depend on HCl content of simulated flue gas. Using a commercial SCR catalyst, they observed adsorption of Hg⁰, with no oxidation, for a simulated flue gas that contained no HCl (at 350°C). The same simulated flue gas with 8 ppm HCl oxidized 95% of the elemental mercury without significant adsorption of mercury (as indicated by loss of total mercury across the catalyst). When HCl was not present in the gas, they observed qualitatively that addition of ammonia resulted in release of adsorbed mercury in the form of Hg⁰.

Data from the multicyclic slipstream reactor at Rockport showed considerable loss of mercury across the commercial catalysts when the catalyst was relatively fresh as illustrated by CEM measurements shown in Figure 13. CEM measurements were made at the inlet to the slipstream reactor and at the outlet of the catalysts. Catalyst C1 was a blank cordierite honeycomb with no active catalyst.

The blank catalyst showed the same amount of mercury at the outlet as at the inlet. Most of the other catalysts, however, showed a loss of mercury across the catalyst. With ammonia on, there was also loss of mercury noted across the commercial catalysts, but not across the blank catalyst C1. This suggests that the catalyst formulation, whether it is in plate or honeycomb form, was responsible for adsorption of mercury. The adsorption was not, however, observed in the second test series after the catalysts had been exposed to flue gas for approximately 2200 hours. Catalysts C5 and C3 oxidized mercury at about the same rate in August as in March/April, whereas catalysts C2, C4 and C6 showed less mercury oxidation in August. The ability of the catalysts to adsorb elemental mercury (or lack thereof) did not seem to be related to the ability of the catalyst to oxidize mercury.

Since adsorption of elemental mercury was observed in laboratory settings and the loss of total mercury (presumably by adsorption) was observed in pilot-scale catalyst, it is reasonable to determine if this phenomenon has been observed at full scale. Figure 27 contains full-scale data on mercury speciation in which the change in elemental mercury across the catalyst is plotted against the change in oxidized mercury. Little or no particulate-bound mercury was reported in the full-scale measurements. Thus, if elemental mercury is oxidized across the SCR, there should be an increase in oxidized mercury that corresponds to the decrease in elemental mercury; the line in the figure denotes this. Most of the full-scale points lie close to the line. There are, however, some full-scale points that lie below the line, suggesting that there may be some adsorption of elemental mercury across the catalysts for certain measurements.

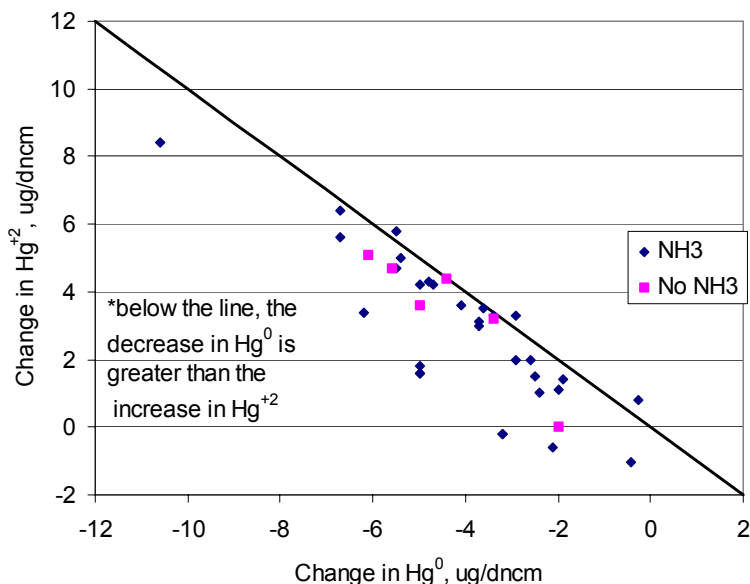


Figure 27. Change in elemental mercury across full-scale SCR catalysts compared with change in oxidized mercury.

The oxidation of elemental mercury across an SCR catalyst therefore does not require a net adsorption of elemental mercury by the catalyst, which could mean that adsorption of elemental mercury is not the rate-limiting step in the process. Since HCl displaces adsorbed mercury (in laboratory experiments), perhaps HCl and Hg^0 are adsorbed on the type of same site.

Laboratory, pilot and full-scale data reviewed in previous quarterly reports have shown that the presence of ammonia reduces the oxidation of elemental mercury. We can suggest a mechanism for the interaction of mercury with SCR catalyst. Elemental mercury is adsorbed on the V_2O_5 sites on the catalyst; the pore structure of the catalyst may influence this adsorption, but there is not enough evidence as yet. HgCl_2 is not adsorbed on the catalyst, although it may be reduced by MoO_3 and WO_3 . Ammonia binds to the vanadium sites on the catalyst as part of the NO reduction process and competes with Hg^0 adsorption. Higher concentrations of HCl in the flue gas result in lower sorption of Hg^0 , perhaps because HCl also reacts with V_2O_5 sites. . Therefore, it seems likely the mercury oxidation process also takes place at the vanadium sites and involves HCl. At this point, there is not enough evidence to determine the detailed mechanism. Several alternatives can be proposed:

1. Hg^0 binds to a vanadium site; HCl binds to an adjacent vanadium site; the reaction takes places between the two bound species.
2. Hg^0 competes with HCl for binding to a vanadium site; bound HCl reacts with gaseous Hg^0 .
3. HCl binds to a vanadium site and forms a chlorinated vanadium compound, which is oxidized (Deacon process) to form Cl_2 , which reactor with Hg^0 in the gas phase.

The Deacon process has been suggested as a means to produce Cl_2 in the gas via reaction between V_2O_5 and HCl.² The gaseous Cl_2 could then react with Hg^0 in the gas phase. The

Deacon process has two steps: adsorption of HCl by the metal oxide to form a chlorinated compound and release of Cl_2 from the chlorinated metal by reaction with oxygen. Experiments by Hisham¹¹ showed that V_2O_5 exposed to HCl in N_2 adsorbed HCl at 150°C and appeared to decompose at 200°C . No release of Cl_2 was noted for reaction of HCl and V_2O_5 in N_2 (as was noted for CuO in the same study). Gutberlet et al.² claimed to have produced Cl_2 across SCR catalysts, but no details were given.

Without further information on the interaction of both HCl and Hg^0 with SCR catalyst, it is not possible to speculate further on a fundamental mechanism. Distinguishing between these alternatives (or elucidating another mechanism) will require detailed laboratory studies.

In the previous quarterly report, thermochemical equilibrium calculations were carried out for flue gas compositions and the speciation of mercury at the inlet and outlet of SCRs was compared to equilibrium predictions. This quarter an error was discovered in the way the previous calculations were set up. The dependence of mercury speciation on HCl concentration was computed incorrectly. Figure 28 shows the corrected equilibrium calculations for the typical bituminous and subbituminous concentrations shown in Table 15.

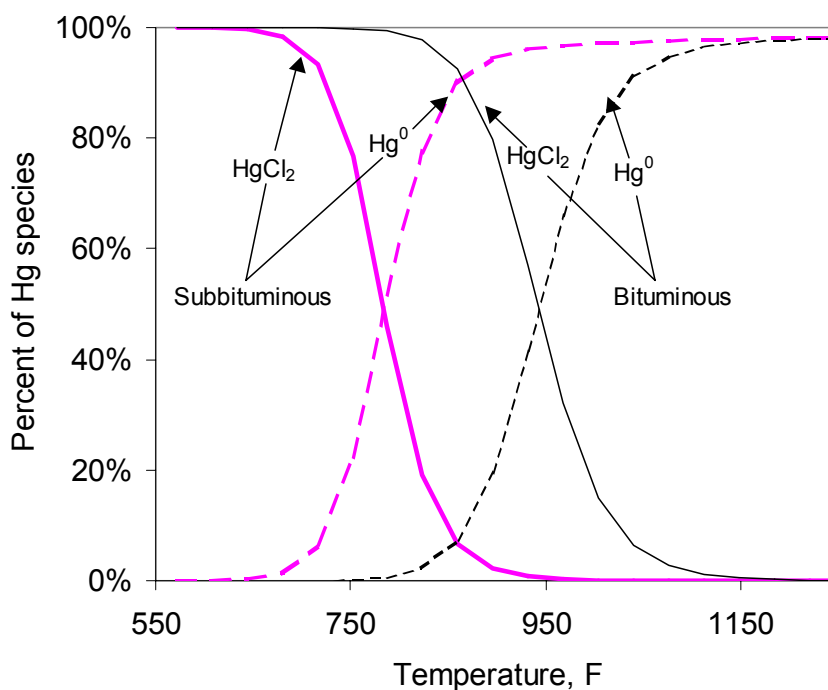


Figure 28. Mercury speciation from thermochemical equilibrium calculations for flue gas compositions from Table 15.

Table 15. Flue gas compositions used for equilibrium calculations.

	Subbit.	Bit.
N ₂ [vol%]	70.6	75.4
CO ₂ [vol%]	13.9	14.6
H ₂ O [vol%]	12.3	6.8
O ₂ [vol%]	3.0	3.0
SO ₂ [ppm]	350	1000
HCl [ppm]	1.75	31
Hg [ppb]	0.2	0.2

At the inlet to the SCR, the mercury in the flue gas is far from equilibrium, as shown in Figure 29, which compares the fraction of elemental mercury at the inlet to the SCR with the equilibrium predictions for various temperatures as a function of the molar chlorine to mercury ratio in the coal. Based on gas-phase kinetic calculations, mercury is not expected to be in equilibrium at the economizer exist. Figure 30 shows the outlet speciation from the same full-scale SCRs. The SCR catalyst has had the effect of rendering mercury at the outlet closer to equilibrium, Yet in full-scale SCRs, mercury in the flue gas does not come to equilibrium.

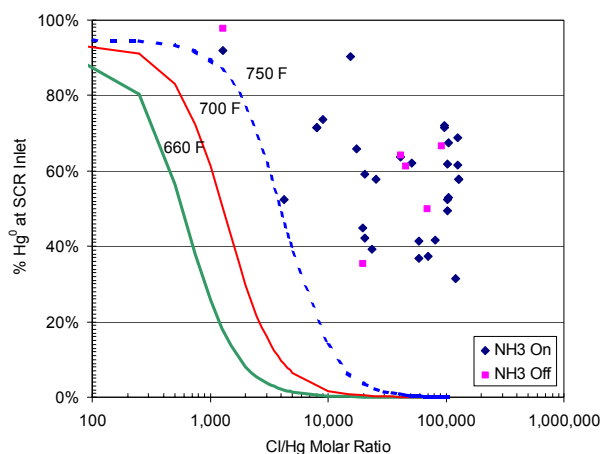


Figure 29. Percentage of mercury as elemental at inlet to SCR: full-scale data compared to equilibrium predictions.

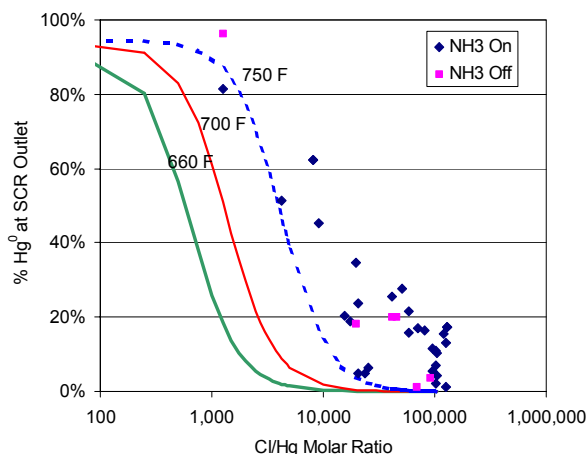


Figure 30. Percentage of mercury as elemental at outlet to SCR: full-scale data compared to equilibrium predictions.

Clearly, a kinetic model is required to describe mercury oxidation across full-scale SCR catalysts. Since the detailed data are not currently available to develop a fundamental reaction mechanism, a global kinetic model will be created and tested against the full-scale data. There is a body of pilot-scale data in the literature⁴⁻⁸, but it details like the inlet mercury concentrations and speciation are not always reported in the literature.

What factors should be incorporated into the global kinetic model? Temperature and space velocity have been shown to be important in laboratory and pilot-scale data discussed in previous quarterly reports. The full-scale data show a correlation between mercury oxidation and temperature as shown in Figure 31. As also observed in pilot-scale data, mercury oxidation decreases with increasing temperature. The scatter in the data suggests that there are other important factors.

HCl concentration is also an important factor, based on laboratory experiments. In Figure 32, the importance of chlorine (as expressed by the coal chlorine content) can be seen for oxidation across full-scale SCRs.

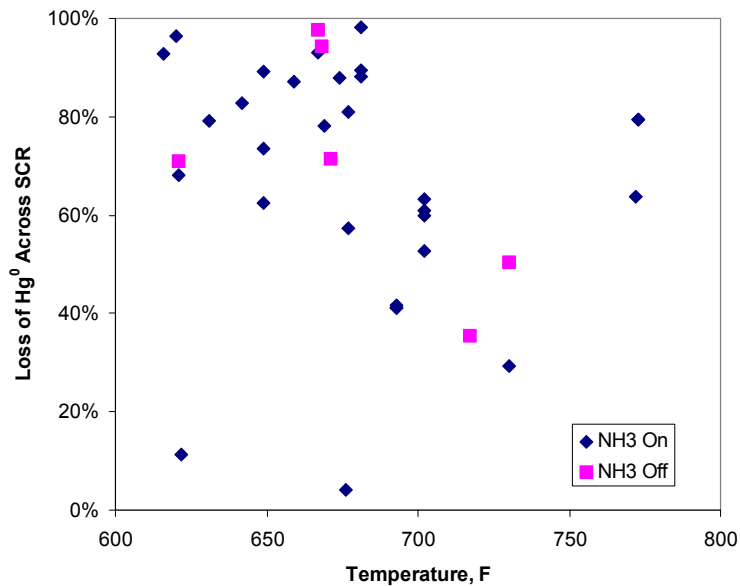


Figure 31. Mercury oxidation across full-scale SCRs as a function of inlet temperature.

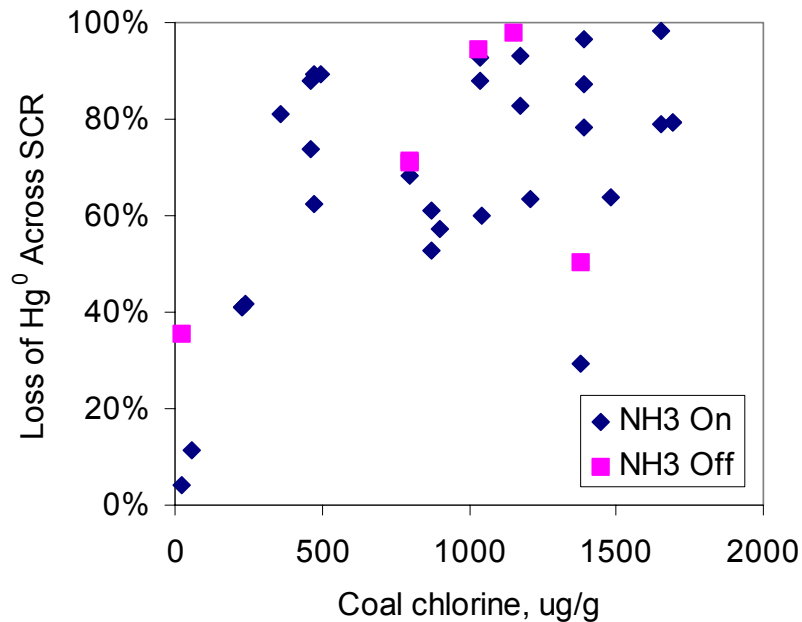


Figure 32. Mercury oxidation across full-scale SCRs as a function of coal chlorine content.

Ammonia has been shown to be important, as discussed above. The available full-scale data contain few measurements without ammonia. Most full-scale SCRs are operated at similar inlet NH_3/NO ratios and with similar amounts of NO removal. Ammonia concentration varies along the length of the reactor and this variation in ammonia will, effectively, be built into the global kinetics.

The full-scale SCR is essentially a plug-flow reactor. As such, integral reactor analysis¹² can be used to develop a global kinetic expression. The conversion of elemental mercury across the SCR is expressed as:

$$X = \frac{[\text{Hg}^0]_{in} - [\text{Hg}^0]_{out}}{[\text{Hg}^0]_{in}} \quad (1)$$

where $[\text{Hg}^0]$ is the concentration of elemental mercury in the flue gas in mol/m^3 . The rate of conversion of mercury per gram of catalyst, R , is:

$$F_{in}X = -R dW \quad (2)$$

where F_{in} is the molar flux of elemental mercury in to the SCR and W is the weight of catalyst in grams. The integral form of Eq. 2 is:

$$\frac{W}{F_{in}} = \int_0^X \frac{dX}{-R} \quad (3)$$

Given an equation for the rate R , Eq. 3 can be integrated to give the conversion at the reactor exit. Based on the evidence discussed previously, the chemical reaction appears to be between Hg^0 and HCl , mediated by active catalyst sites. The simplest rate equation can be written as

$$-R = k[\text{HCl}][\text{Hg}^0] \quad (4)$$

Substituting Eq. 4 into Eq. 3 and integrating gives:

$$k \frac{W[\text{HCl}][\text{Hg}^0]_{in}}{F_{in}} = \ln\left(\frac{1}{1-X}\right) \quad (5)$$

In doing so, the concentration of HCl has been assumed to be constant across the SCR. Considering the large excess of HCl with respect to mercury, this seems reasonable. Thus, if we plot the quantity $\frac{W[\text{HCl}][\text{Hg}^0]_{in}}{F_{in}}$ against $\ln\left(\frac{1}{1-X}\right)$, the slope should be equal to the rate constant k . This plot is shown in Figure 33. Full-scale data have been included that were taken with the ammonia on and for which the loss of total mercury across the catalyst was less than 20 per cent. That is, if there was an apparent loss of total mercury across the catalyst, then the data should be considered suspect. The data points have been divided into temperature ranges. Table 16 gives the values of the slopes of the lines. For three of the four temperature ranges, reasonable fits to the data were obtained. Figure 34 displays the data points without ammonia. Although the fitted rate constant without ammonia is higher than the rate constant with ammonia for the same temperature range, there appears to be overlap in the data points. It is difficult to conclude that the two sets of data points are different. More full-scale data without ammonia are needed.

Table 16. Rate constants derived from full-scale data.

T, °F	616-631	642-659	667-681	693-702	667-681*
$k, (m^6/mol^2)/(g-s)$	3.25E+09	4.86E+09	6.05E+09	4.35E+09	7.98E+09
r^2	0.544	-3.102	0.325	0.565	0.610

* No ammonia

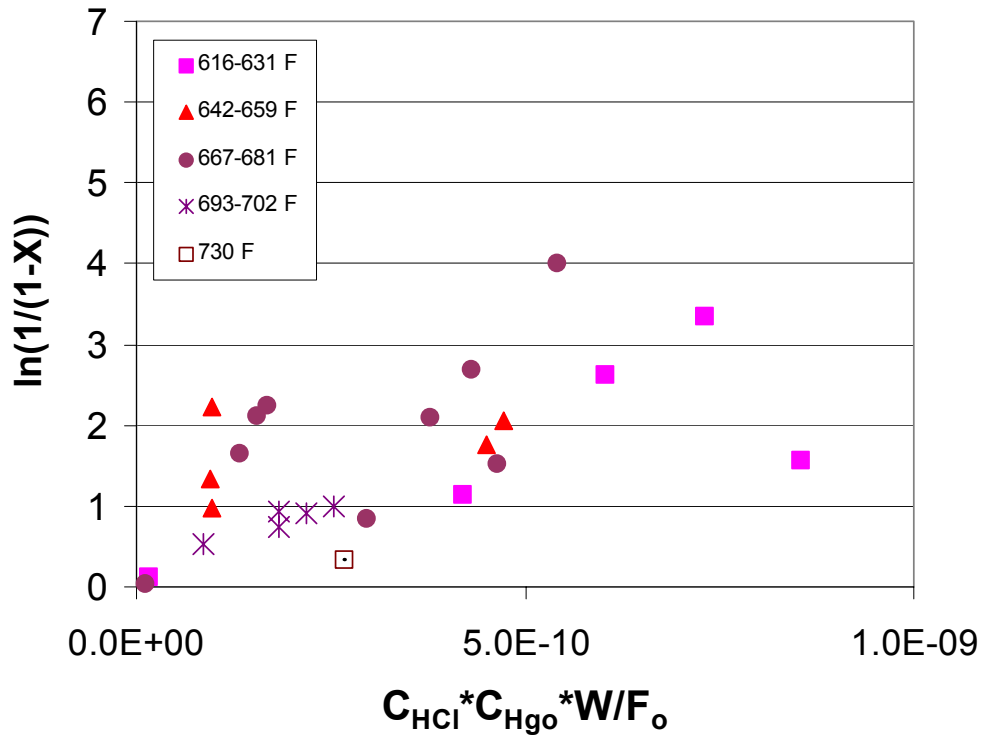


Figure 33. $\frac{W[HCl][Hg^0]_{in}}{F_{in}}$ vs. $\ln\left(\frac{1}{1-X}\right)$ from full-scale data with ammonia.

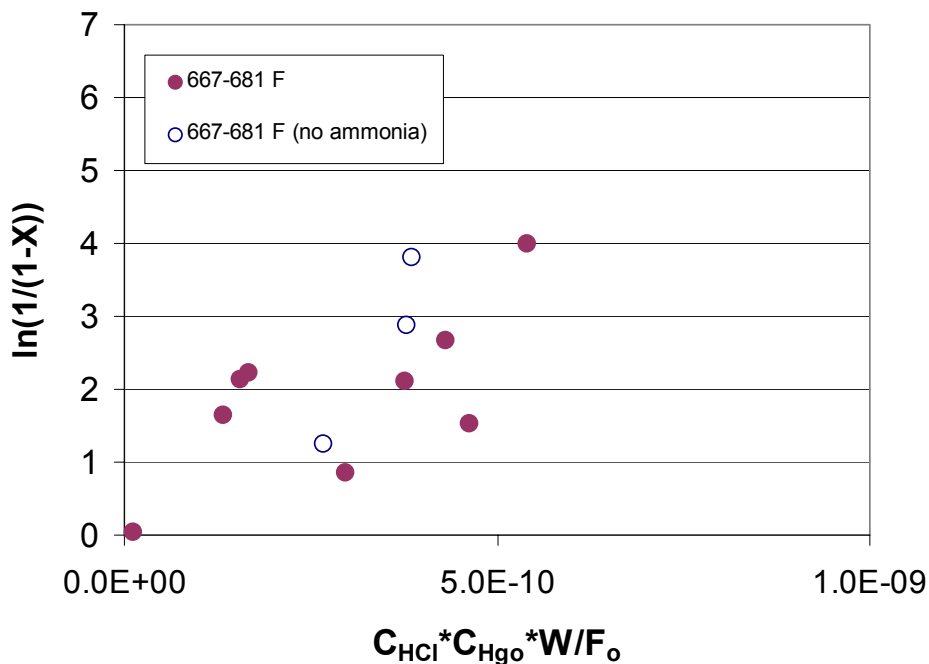


Figure 34. $\frac{W[HCl][Hg^0]_{in}}{F_{in}}$ vs. $\ln\left(\frac{1}{1-X}\right)$ from full-scale data with and without ammonia, 667-681°F.

Based on full-scale data, a global kinetic model has been created for mercury oxidation. This model is applicable to full-scale SCRs that inject ammonia at NH_3/NO ratios that are typical of commercial operation. Figure 35 shows two examples of how the model could be used.

(a) Effect of load changes

Changing load in the boiler decreases the amount of flue gas, increasing the residence time in the SCR, and drops the temperature in the SCR. Both will have an effect on Hg oxidation across the catalyst. Assume a plant burning a bituminous coal with $800 \mu\text{g/g Cl}$ and $0.011 \mu\text{g/g Hg}$. The SCR is a plate catalyst. At full load, the space velocity is 2000 hr^{-1} and the temperature is 700°F . Assume that at 70% load, the space velocity is 1500 hr^{-1} and the temperature is 675°F . Under these conditions, the model predicts an increase in Hg oxidation from 70 per cent to 90 percent.

(b) Effect of blending

When the primary fuel for a boiler is a subbituminous or lignite coal, a potentially inexpensive way to increase the HCl in the flue gas is to blend in a higher chlorine bituminous coal. Assume that the SCR design and operation are the same as in example (a). The subbituminous coal has $25 \mu\text{g/g Cl}$ and $0.011 \mu\text{g/g Hg}$, while the bituminous coal is the same as in example (a). Blending

bituminous coal with subbituminous coal increases mercury oxidation, in this example, from about 5 percent up to 40 percent (at 60% subbituminous coal).

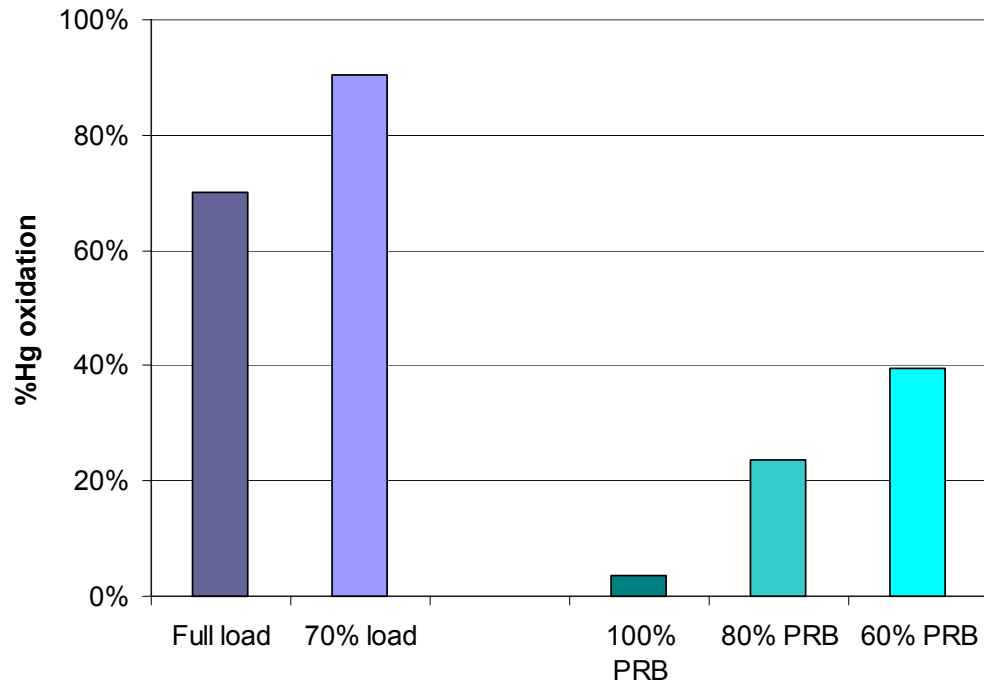


Figure 35. Calculated Hg oxidation across full-scale SCRs; see text for details.

Conclusions

Five commercial catalysts and one blank monolith were exposed to flue gas from a blend of 87% subbituminous coal and 13% eastern bituminous coal. Mercury measurements were carried out when the catalysts were relatively new, corresponding to about 300 hours of operation and again after 2,200 hours of operation. NO_x , O_2 and gaseous mercury speciation at the inlet and at the outlet of each catalyst chamber were measured. In general, the catalysts all appeared capable of achieving about 90% NO_x reduction at a space velocity of $3,000 \text{ hr}^{-1}$ when new, which is typical of full-scale installations; after 2,200 hours exposure to flue gas, some of the catalysts appeared to lose NO_x activity. Fresh commercial catalysts showed mercury oxidation that was in the range of 25 % to 65 % at typical full-scale space velocities, consistent with observed full-scale oxidation in bituminous coal flue gas, even though the blend was predominantly subbituminous coal. However, the chlorine content of the blend (100 to 240 $\mu\text{g/g}$ on a dry basis) was higher than typical values for subbituminous coals. A blank monolith showed no oxidation of mercury under any conditions. All catalysts showed higher mercury oxidation without ammonia, consistent with full-scale measurements. After exposure to flue gas for 2,200 hours, some of the catalysts showed reduced levels of mercury oxidation relative to the initial levels of oxidation.

A review of the available data on mercury oxidation across SCR catalysts from small, laboratory-scale experiments, pilot-scale slipstream reactors and full-scale power plants was carried out. SCR catalysts are, under certain circumstances, capable of driving mercury speciation toward the gas-phase equilibrium values at the SCR temperature. However, evidence suggests that mercury does not reach equilibrium at the outlet of SCR catalysts. Some of the other factors that have been shown to affect mercury chemistry across SCR catalysts are the space velocity and the presence of ammonia. There may be other factors, such as the sulfur content of the coal, that become apparent as more data become available. Catalyst properties may be important, including: the mix between vanadium oxides and other oxides in the catalyst; the pore size distribution; and catalyst deactivation with time.

A global kinetic model of Hg oxidation across SCRs was formulated based on full-scale data. The model took into account the effects of temperature, space velocity, catalyst type and HCl concentration in the flue gas. The results of this analysis suggest strategies for maximizing the amount of oxidized mercury at the exit of SCR catalysts. The chief of these is to increase the chlorine content of the flue gas, either through blending low-chlorine coal with high-chlorine coal or additives. Lowering the temperature is another option, but this may not be practical in many utility boilers. Furthermore, NO reduction across SCR catalysts decreases with temperature.

Acknowledgements

We are grateful to Carl Richardson, Mandi Richardson, Tom Machalek and Julie Range from URS Corporation for the mercury measurements made in the field. We are also very grateful to Steve Pfeister, Gary Spitznogle, Aimee Toole, and Anja Vesanen of American Electric Power for providing invaluable help in logistics, planning and data collection.

References

1. Lee, C.W., Srivastava, R.K., Ghorishi, S.B., Hastings, T.W., Stevens, F.M. "Study of Speciation of Mercury under Simulated SCR NO_x Emission Control Conditions," presented at the DOE-EPRI-U.S. EPA -A&WMA Combined Power Plant Air Pollutant Control Symposium - The Mega Symposium, Washington, DC, May 19-22, 2003.
2. Gutberlet, H., Schlüter, A., Licata, A. "SCR Impacts on Mercury Emissions from Coal-Fired Boilers," presented at EPRI SCR Workshop, Memphis, TN, April 19-21, 2000.
3. Hocquel, M., "The Behaviour and Fate of Mercury in Coal-Fired Power Plants with Downstream Air Pollution Control Devices" *Forsch.-Ber. VDI Reihe Nr. 251*. Düsseldorf: VDI Verlag 2004.
4. Richardson, C., Machalek, T., Miller, S., Dene, C., Chang, R. "Effect of NO_x Control Processes on Mercury Speciation in Flue Gas," presented at the Air Quality III Meeting, Washington, D.C., September 10-13, 2002.
5. Laudal, D.L., Pavlish, J.H., Chu, P., "Pilot-Scale Evaluation of the Impact of Selective Catalytic Reduction for NO_x on Mercury Speciation," paper presented at the Air & Waste Management Association 94th Annual Conference, Orlando, Florida, June 24-28, 2001.
6. Machalek, T., Ramavajjala, M., Richardson, M., Richardson, Dene, C., Goeckner, B., Anderson, H., Morris, E., "Pilot Evaluation of Flue Gas Mercury Reactions Across an SCR Unit," presented at the DOE-EPRI-U.S. EPA -A&WMA Combined Power Plant Air Pollutant Control Symposium - The Mega Symposium, Washington, DC, May 19-22, 2003.
7. Richardson, C., Machalek, T., Miller, S., Dene, C., Chang, R. "Effect of NO_x Control Processes on Mercury Speciation in Utility Flue Gas" *J. Air Waste Manage. Assoc.*, **2002**, 52, 941-947
8. Laudal, D. *Effect of Selective Catalytic Reduction on Mercury, 2002 Field Studies Update*, EPRI, Palo Alto, CA: 2002. Product ID 1005558.
9. Chu, P., Laudal, D., Brickett, L., Lee, C.W. "Power Plant Evaluation of the Effect of SCR Technology on Mercury," presented at the DOE-EPRI-U.S. EPA -A&WMA Combined Power Plant Air Pollutant Control Symposium - The Mega Symposium, Washington, DC, May 19-22, 2003.
10. La Marca, C., Cioni, M., Pintus, N., Rossi, N., Malloggi, S., Barbieri, A. "Macro and Micro-Pollutant Emission Reduction in Coal-Fired Power Plant," presented at Seventh International Conference on Energy for a Clean Environment (Clean Air 2003), Lisbon, Portugal, July 7-10, 2003.
11. Hisham, M. W. M. and Benson, S.W. "Thermochemistry of the Deacon Process," *J. Phys. Chem.* **1995**, 99, 6194-6198.
12. Levenspiel, O. *Chemical Reaction Engineering*, Second Edition, John Wiley and Sons, New York: 1972.
13. Merriam, N. W., Grimes, R. W., Tweed, R. E., "Process for low mercury coal," United States Patent 5,403,365, April 4, 1995.

Appendix A
Full-Scale Data

Table A.1. Full-scale data without ammonia.

Boiler	Capacity, MW	SCR Catalyst Type	SCR Space velocity, 1/hr	Coal Rank	Coal, Hg ug/g (dry)	Coal, Cl ug/g (dry)	SCR Inlet, ug/dNm ³ at 3% O ₂					SCR Outlet, ug/dNm ³ at 3% O ₂					%Loss - SCR		%Hg ⁰	
							Temp., °F	Hg _{Total}	Hg _P	Hg ⁺²	Hg ⁰	Temp., °F	Hg _{Total}	Hg _P	Hg ⁺²	Hg ⁰	Hg _{Total}	Hg ⁰	SCR Inlet	SCR Outlet
B3	900	plate	1515	Bit.	0.11	800	621	13.4	N.R.	4.8	8.6	N.R.	12.4	N.R.	9.9	2.5	7.5%	70.9%	64.2%	20.2%
B3	1300	plate	2188	Bit.	0.095	1152	667	9	N.R.	4.5	4.5	N.R.	9	N.R.	8.9	0.1	0.0%	97.8%	50.0%	1.1%
B5	1300	plate	1990	Bit.	0.064	1032	668	5.4	N.R.	1.9	3.6	N.R.	5.3	N.R.	5.1	0.2	1.9%	94.4%	66.7%	3.8%
B3	1300	plate	2188	Bit.	0.10	800	671	11.4	N.R.	4.4	7	N.R.	10	N.R.	8	2	12.3%	71.4%	61.4%	20.0%
S1	600	honeycomb	1800	Subbit.	0.102	23	717	5.72	N.R.	0.12	5.6	N.R.	3.76	N.R.	0.14	3.62	34.3%	35.4%	97.9%	96.3%
S3	750	honey comb	3930	Bit.	0.4	1380	730	31.2	N.R.	20.1	11.1	751	30.3	N.R.	24.8	5.5	2.9%	50.5%	35.6%	18.2%

N.R. – Not reported

Table A.2. Full-scale data with ammonia on.

Boiler	Capacity, MW	SCR Catalyst Type	Space velocity, 1/hr	Coal Rank	Coal, Hg ug/g (dry)	Coal, Cl, ug/g (dry)	SCR Inlet, ug/dNm ³ at 3% O ₂					SCR Outlet, ug/dNm ³ at 3% O ₂					%Loss - SCR		%Hg ⁰	
							Temp., °F	Hg _{Total}	Hg _P	Hg ⁺²	Hg ⁰	Temp., °F	Hg _{Total}	Hg _P	Hg ⁺²	Hg ⁰	Hg _{Total}	Hg ⁰	SCR Inlet	SCR Outlet
B5	900	plate	1378	Bit.	0.056	1036	616	5.3	N.R.	2.5	2.8	N.R.	4.7	N.R.	4.5	0.2	11.3%	92.9%	52.8%	4.3%
B3	900	plate	1515	Bit.	0.076	1389	620	9.2	N.R.	3.5	5.7	N.R.	9.5	N.R.	9.3	0.2	-3.3%	96.5%	62.0%	2.1%
B3	900	plate	1515	Bit.	0.11	800	621	14.3	N.R.	5.2	9.1	N.R.	11.4	N.R.	8.6	2.9	20.3%	68.1%	63.6%	25.4%
E1	320	honeycomb	3420	Bit.	0.080	60	621.8	6.96	N.R.	1.76	3.65	621.8	6.3	N.R.	0.74	3.24	9.5%	11.2%	52.4%	51.4%
B3	900	plate	1515	Bit.	0.075	1655	631	7	N.R.	2.7	4.3	N.R.	6.9	N.R.	6	0.9	1.4%	79.1%	61.4%	13.0%
B5	1304	plate	1990	Bit.	0.069	1173	642	4.9	N.R.	1.4	3.5	N.R.	5.2	N.R.	4.7	0.6	-6.1%	82.9%	71.4%	11.5%
S5	684	plate	3700	Bit.	0.13	472	649	13.3	0.16	7.5	5.6	653	12.4	0.07	11.7	0.6	6.8%	89.3%	42.1%	4.8%
S5	684	plate	3700	Bit.	0.13	472	649	14.9	0.08	6	8.8	653	14	0.04	10.7	3.3	6.0%	62.5%	59.1%	23.6%
S5	684	plate	3700	Bit.	0.15	460	649	13.8	0.04	4.7	9.1	653	12.7	0.02	10.3	2.4	8.0%	73.6%	65.9%	18.9%
B3	1300	plate	2188	Bit.	0.076	1389	659	10.5	N.R.	5	5.5	N.R.	10	N.R.	9.3	0.7	4.8%	87.3%	52.4%	7.0%
B5	1304	plate	1990	Bit.	0.069	1173	667	6.1	N.R.	1.7	4.4	N.R.	5.6	N.R.	5.3	0.3	8.2%	93.2%	72.1%	5.4%
B3	1300	plate	2188	Bit.	0.076	1389	669	9.3	N.R.	4.7	4.6	N.R.	9.1	N.R.	8.2	1	2.2%	78.3%	49.5%	11.0%
B5	1300	plate	1990	Bit.	0.056	1036	674	4.9	N.R.	1.6	3.3	N.R.	3.9	N.R.	3.6	0.4	20.4%	87.9%	67.3%	10.3%
S1	600	honeycomb	1800	Subbit.	0.102	23	676	6.69	0.01	0.52	6.15	N.R.	7.22	0.01	1.31	5.89	-7.9%	4.2%	91.9%	81.6%
B3	1300	plate	2188	Bit.	0.10	900	677	13.2	N.R.	5	8.2	N.R.	12.7	N.R.	9.2	3.5	3.8%	57.3%	62.1%	27.6%
S4	650	honeycomb	2275	Bit.	0.131	360	677	14.5	N.R.	1.4	13.1	669	12.3	N.R.	9.8	2.5	15.2%	80.9%	90.3%	20.3%
B3	1300	plate	2188	Bit.	0.075	1655	681	8	N.R.	2.5	5.5	N.R.	7.6	N.R.	7.5	0.1	5.0%	98.2%	68.8%	1.3%
S2	1360	plate	2125	Bit.	0.11	498	681	13	0.09	5.4	7.5	656	12.6	0.03	11.8	0.8	3.1%	89.3%	57.7%	6.3%
S2	1360	plate	2125	Bit.	0.11	459	681	10.7	0.03	6.5	4.2	656	10.1	0.02	9.5	0.5	5.6%	88.1%	39.3%	5.0%
S4	700	honeycomb	2275	Bit.	0.16	228	693	10.9	0.11	3	7.8	692	7.4	0	2.8	4.6	32.1%	41.0%	71.6%	62.2%
S4	700	honeycomb	2275	Bit.	0.16	228	693	10.9	0.11	3	7.8	692	7.4	0	2.8	4.6	32.1%	41.0%	71.6%	62.2%
S4	700	honeycomb	2275	Bit.	0.15	241	693	12.1	0	3.2	8.9	692	11.5	0	6.3	5.2	5.0%	41.6%	73.6%	45.2%
S6	700	honeycomb	3800	Bit.	0.084	1210	702	7.2	0.03	4.1	3	701	6.7	0.03	5.5	1.1	6.9%	63.3%	41.7%	16.4%
S6	700	honeycomb	3800	Bit.	0.084	1041	702	10.7	0.05	6.7	4	701	9.4	0.04	7.7	1.6	12.1%	60.0%	37.4%	17.0%
S6	700	honeycomb	3800	Bit.	0.084	871	702	9.2	<0.1	5.5	3.8	701	8.3	<0.1	6.6	1.8	9.8%	52.6%	41.3%	21.7%
S6	700	honeycomb	3800	Bit.	0.084	871	702	11.1	<0.1	7	4.1	701	10.2	0.01	8.5	1.6	8.1%	61.0%	36.9%	15.7%
S3	750	honeycomb	3930	Bit.	0.4	1380	730	37.9	N.R.	20.9	17	751	34.7	N.R.	22.7	12.0	8.4%	29.4%	44.9%	34.6%
B4	650	honeycomb	5252	Bit.	0.07	1479	772	10.5	<0.1	7.2	3.3	751	7.8	<0.1	6.6	1.2	25.7%	63.6%	31.4%	15.4%
B4	650	honeycomb	5252	Bit.	0.07	1694	773	10.9	<0.1	4.6	6.3	751	7.5	<0.1	6.2	1.3	31.2%	79.4%	57.8%	17.3%
B4	650	honeycomb	5252	Bit.	0.07	1694	773	10.9	<0.1	4.6	6.3	751	7.5	<0.1	6.2	1.3	31.2%	79.4%	57.8%	17.3%

Appendix B

Catalyst NO_x Data from Slipstream Reactor

The NO_x concentration at the inlet is calculated at 5% O₂. The inlet concentration has been interpolated based on measurements of the inlet concentration made before and after the measurement of the NO_x concentration at the outlet of each chamber. The ammonia concentration was calculated at 5% O₂, based on the total flow measured in the slipstream reactor and the set point of the ammonia mass flow controller. The NH₃/NO ratio is calculated from the ammonia concentration divided by the estimated inlet NO_x concentration. The average catalyst chamber temperature is calculated from the average of the temperature before the catalyst and at the exit of the catalyst chamber. The space velocity is calculated at 32°F (0°C).

Table B.1. NO_x data for catalyst C1 (blank monolith).

Chamber	Date	Inlet NO _x ppm (est)	NO _x reduc.	T before cat, °F	NH ₃ /NO	Avg T catal, °F	SV, hr ⁻¹
one	3/26/03	329	6.1%	655	1.40	625	6,279
one	3/27/03	318	3.1%	662	1.35	634	6,283
one	8/11/03	334.5	6.1%	617	1.02	555	2,745
one	8/12/03	332.7	-0.3%	678	1.05	602	1,406
one	8/13/03	318.9	3.1%	617	0.94	553	1,803
one	8/21/03	392.5	-4.8%	696	0.88	654	4,050
one	8/21/03	383.3	1.8%	698	1.00	655	4,126
one	8/21/03	370.7	5.7%	691	1.23	647	4,225
one	8/21/03	373.4	12.8%	691	1.25	646	4,242

Table B.2. NO_x data for catalyst C2 (monolith).

Chamber	Date	Inlet NO _x ppm (est)	NO _x reduc.	T before cat, °F	NH ₃ /NO	Avg T catal, °F	SV, hr ⁻¹
two	3/26/03	329.4	83.2%	657	1.43	627	7064
two	3/27/03	323.8	83.8%	662	1.43	628	7,087
two	3/27/03	335.9	85.4%	662	1.32	629	7,080
two	3/27/03	311.8	85.7%	655	1.32	623	7,073
two	3/27/03	308.5	83.5%	660	1.40	630	7,119
two	3/27/03	328.6	85.1%	658	1.29	628	7,076
two	3/27/03	239.6	78.4%	668	1.62	649	7,099
two	3/27/03	317.0	83.6%	667	1.26	648	7,093
two	4/5/03	301.4	83.8%	685	1.27	648	8510
two	4/5/03	301.4	83.7%	685	1.27	646	8501
two	8/11/03	334.5	71.4%	617	1.02	554	5,687
two	8/12/03	331.7	76.7%	644	1.20	570	3,568
two	8/13/03	318.9	62.2%	611	0.93	553	4,841
two	8/15/03	331.4	70.7%	612	1.23	543	5,125
two	8/21/03	383.6	74.8%	694	0.94	658	8,682
two	8/21/03	391.2	75.4%	698	0.94	661	8,654
two	8/21/03	382.7	75.4%	698	1.14	661	8,641
two	8/21/03	378.1	74.5%	692	1.16	656	8,696
two	8/21/03	371.1	73.5%	691	1.29	654	8,756
two	8/21/03	373.4	73.6%	691	1.27	654	8,751
two	8/22/03	361.6	72.2%	674	0.94	636	8,656
two	8/22/03	350.5	70.9%	678	0.92	641	8,800
two	8/22/03	337.5	69.2%	676	0.89	640	8,859
two	8/22/03	344.9	70.1%	683	0.92	645	8,967
two	8/22/03	365.7	72.0%	690	0.97	653	8,963
two	8/22/03	364.2	71.5%	690	0.96	654	8,973
two	8/22/03	345.5	70.6%	689	1.00	653	8,940
two	8/22/03	362.3	72.5%	690	0.98	654	8,837
two	8/22/03	351.9	71.2%	688	0.96	652	8,878

Table B.3. NO_x data for catalyst C3 (plate).

Chamber	Date	Inlet NO _x ppm (est)	NO _x reduc.	T before cat, °F	NH ₃ /NO	Avg T catal, °F	SV, hr ⁻¹
three	3/26/03	311.3	93.0%	658	1.48	646	3,113
three	3/27/03	324.0	92.8%	661	1.41	648	3,092
three	3/27/03	329.9	91.4%	665	1.21	652	3,105
three	3/27/03	309.4	91.2%	653	1.34	641	3,103
three	3/27/03	319.1	90.7%	659	1.34	649	3,092
three	3/27/03	327.4	92.0%	656	1.29	646	3,127
three	3/27/03	319.2	92.0%	661	1.52	651	3,101
three	3/27/03	318.7	89.3%	667	1.27	662	3,085
three	3/27/03	316.7	88.4%	668	1.27	663	3,103
three	4/5/03	301.4	97.2%	685	1.27	666	3,120
three	8/16/03	349.1	56.8%	599	3.44	573	1,115
three	8/12/03	331.7	71.5%	678	0.97	652	2,583
three	8/13/03	318.9	64.7%	610	0.92	591	2,587
three	8/11/03	334.5	74.5%	619	1.01	600	2,599
three	8/16/03	349.1	84.2%	645	1.06	631	3,715
three	8/22/03	351.4	78.7%	688	0.97	673	5,251
three	8/22/03	363.3	79.9%	689	0.98	674	5,267
three	8/21/03	390.0	81.6%	700	1.02	683	5,293
three	8/21/03	382.0	81.5%	698	1.17	682	5,298
three	8/21/03	384.1	81.0%	695	0.95	679	5,322
three	8/21/03	377.0	80.3%	693	1.19	677	5,325
three	8/22/03	343.9	78.3%	690	1.01	674	5,330
three	8/21/03	371.4	80.0%	692	1.28	675	5,339
three	8/21/03	373.4	79.7%	692	1.24	675	5,345
three	8/22/03	365.9	79.3%	690	0.96	673	5,373
three	8/22/03	336.2	76.7%	678	0.90	659	5,409
three	8/22/03	366.2	79.5%	690	0.97	673	5,421
three	8/22/03	351.6	78.2%	679	0.92	661	5,438
three	8/22/03	342.9	77.1%	685	0.92	667	5,446
three	8/22/03	363.0	78.6%	677	0.93	658	5,464
three	8/21/03	407.5	82.5%	695	0.27	679	5,334

Table B.4. NO_x data for catalyst C4 (plate).

Chamber	Date	Inlet NO _x ppm (est)	NO _x reduc.	T before cat, °F	NH ₃ /NO	Avg T catal, °F	SV, hr ⁻¹
four	3/26/03	312.0	92.1%	663	1.31	650	2,154
four	3/27/03	324.4	94.5%	660	1.37	647	2,148
four	3/27/03	322.4	94.6%	661	1.32	648	2,158
four	3/27/03	307.7	94.3%	658	1.45	644	2,147
four	3/27/03	336.4	94.8%	659	1.26	647	2,154
four	3/27/03	326.4	94.8%	656	1.36	645	2,152
four	3/27/03	328.3	94.1%	663	1.46	654	2,984
four	3/27/03	325.0	87.0%	669	1.28	665	3,064
four	4/5/03	301.4	88.8%	685	1.27	676	6007
four	4/5/03	301.4	61.3%	489	1.26	456	6001
four	8/12/03	331.7	75.1%	617	1.19	605	2,541
four	8/13/03	318.9	64.0%	626	0.91	615	2,669
four	8/22/03	350.8	86.9%	686	0.97	673	3,196
four	8/22/03	364.3	87.4%	690	0.98	677	3,220
four	8/22/03	342.3	86.2%	691	1.02	677	3,224
four	8/22/03	366.7	86.3%	689	0.97	676	3,325
four	8/22/03	367.5	87.2%	690	0.95	677	3,421
four	8/22/03	352.7	84.9%	680	0.93	666	3,917
four	8/22/03	340.8	84.4%	686	0.93	671	4,012
four	8/22/03	364.4	84.9%	678	0.93	663	4,031
four	8/22/03	335.0	83.3%	676	0.92	663	4,059
four	8/11/03	334.5	79.8%	617	1.02	603	4,169
four	8/21/03	376.0	87.2%	693	1.32	679	4,170
four	8/21/03	371.7	86.7%	692	1.27	678	4,216
four	8/21/03	389.0	87.8%	701	1.04	685	4,235
four	8/21/03	381.3	87.4%	697	0.85	683	4,250
four	8/21/03	384.5	87.4%	695	0.94	680	4,250
four	8/21/03	373.4	86.5%	691	1.18	676	4,323
four	8/21/03	405.1	88.3%	696	0.53	681	4,308

Table B.5. NO_x data for catalyst C5 (monolith).

Chamber	Date	Inlet NO _x ppm (est)	NO _x reduc.	T before cat, °F	NH ₃ /NO	Avg T catal, °F	SV, hr ⁻¹
five	3/26/03	330.9	88.3%	663	1.39	638	6988
five	3/27/03	320.0	90.4%	663	1.32	637	6,997
five	3/27/03	321.6	88.9%	660	1.25	635	7,026
five	3/27/03	303.5	89.2%	659	1.44	633	7,068
five	3/27/03	334.6	89.1%	658	1.29	635	7,016
five	3/27/03	326.9	88.5%	656	1.40	633	6,977
five	3/27/03	333.1	98.4%	663	1.36	641	7,021
five	3/27/03	328.7	79.7%	663	1.23	649	6,993
five	3/27/03	313.8	85.7%	668	1.31	656	7,047
five	4/5/03	301.4	83.2%	684	1.27	646	10772
five	4/5/03	301.4	67.2%	528	1.27	457	10924
five	8/12/03	331.7	72.4%	607	1.19	543	3,635
five	8/13/03	318.9	66.1%	608	0.92	547	4,564
five	8/16/03	349.1	68.0%	645	1.18	604	6,973
five	8/21/03	385.0	90.7%	695	0.94	665	9,742
five	8/21/03	402.9	90.7%	697	0.79	667	9,742
five	8/21/03	387.9	90.6%	698	1.06	669	9,743
five	8/21/03	380.6	90.7%	696	1.01	667	9,741
five	8/21/03	375.3	90.6%	694	1.23	663	9,740
five	8/21/03	371.9	90.3%	692	1.28	662	9,741
five	8/21/03	373.4	90.9%	691	1.15	660	9,743
five	8/22/03	365.9	89.6%	677	0.94	646	9,740
five	8/22/03	353.9	89.3%	680	0.93	649	9,738
five	8/22/03	333.7	88.3%	677	0.91	646	9,743
five	8/22/03	338.7	88.5%	686	0.94	654	9,741
five	8/22/03	367.2	89.6%	689	0.96	658	9,744
five	8/22/03	369.2	89.5%	689	0.95	658	9,742
five	8/22/03	340.7	89.3%	691	1.02	660	9,743
five	8/22/03	365.2	90.3%	691	0.98	660	9,739
five	8/22/03	350.3	89.4%	685	0.98	656	9,740
five	8/16/03	349.1	58.7%	608	3.75	544	2,593

Table B.6. NO_x data for catalyst C6 (monolith).

Chamber	Date	Inlet NO _x ppm (est)	NO _x reduc.	T before cat, °F	NH ₃ /NO	Avg T catal, °F	SV, hr ⁻¹
six	3/26/03	324.0	81.6%	660	1.41	632	7198
six	3/27/03	313.1	79.9%	663	1.31	633	7,174
six	3/27/03	320.2	81.3%	663	1.34	632	7,191
six	3/27/03	309.7	79.2%	658	1.40	629	7,208
six	3/27/03	325.9	79.3%	655	1.35	628	7,213
six	3/27/03	334.3	81.5%	667	1.45	641	7,170
six	4/5/03	301.4	70.4%	684	1.27	649	10745
six	4/5/03	301.4	67.7%	554	1.28	494	10737
six	8/12/03	331.7	64.4%	603	1.22	555	2,219
six	8/13/03	318.9	58.2%	613	0.93	566	2,314
six	8/21/03	387.9	86.2%	695	0.94	673	9,619
six	8/21/03	400.9	86.2%	696	0.79	674	9,632
six	8/21/03	386.9	85.8%	697	1.04	675	9,606
six	8/21/03	379.9	85.9%	694	1.19	673	9,611
six	8/21/03	374.7	86.2%	693	1.30	671	9,615
six	8/21/03	372.1	86.0%	693	1.27	671	9,631
six	8/22/03	367.3	88.2%	676	0.92	655	9,614
six	8/22/03	355.0	87.1%	679	0.92	657	9,631
six	8/22/03	332.5	83.9%	679	0.92	657	9,660
six	8/22/03	336.5	85.7%	687	0.98	665	9,618
six	8/22/03	367.7	87.6%	689	0.97	668	9,623
six	8/22/03	370.9	88.3%	687	0.94	667	9,639
six	8/22/03	339.1	87.0%	691	1.03	670	9,630
six	8/22/03	366.2	88.9%	691	0.98	670	9,640
six	8/22/03	349.7	88.3%	685	0.98	664	9,603
six	8/22/03	357.7	80.6%	685	0.98	662	9,626
six	8/22/03	364.5	79.1%	691	0.98	669	9,634

Appendix C

Catalyst Mercury Data from Slipstream Reactor

Table C.1. Averaged mercury data from first test series.

Start Time	End Time	Chamber	Tcab-avg, °F	SV, hr ⁻¹	NH ₃ , ppm	NH ₃ /NO	Species	Hg, ug/dscm	Hg St. Dev.
3/28/03 9:17	9:47	inlet			531	1.71	elemental	5.68	0.19
3/28/03 9:48	10:18	one	659	2538	527	1.70	elemental	5.77	0.34
3/28/03 10:18	10:48	two	661	5030	525	1.69	elemental	4.21	0.16
3/28/03 11:20	11:50	inlet			530	1.71	elemental	5.53	0.20
3/28/03 13:23	13:53	inlet			535	1.73	elemental	5.62	0.30
3/28/03 13:53	14:16	inlet			589	1.90	elemental	5.10	0.24
3/28/03 16:18	17:03	two	659	5064	543	1.75	elemental	3.77	0.26
3/28/03 17:05	17:20	inlet			581	1.87	total	7.63	0.23
3/28/03 17:20	17:35	one	654	2097	579	1.87	total	7.68	0.36
3/28/03 17:50	18:05	four	654	2395	606	1.96	total	6.69	0.37
3/31/03 12:37	12:57	inlet			660	2.13	elemental	5.16	0.51
3/31/03 12:57	13:17	one	657	2124	619	2.00	elemental	8.03	0.16
3/31/03 13:17	13:37	two	658	5037	633	2.04	elemental	4.85	0.25
3/31/03 13:37	13:57	three	661	1927	644	2.08	elemental	4.99	1.02
3/31/03 13:59	14:19	inlet			625	2.01	elemental	5.19	0.54
3/31/03 14:20	14:39	four	655	2400	627	2.02	elemental	2.56	0.08
3/31/03 14:40	15:00	five	655	2259	625	2.02	elemental	3.90	1.20
3/31/03 15:00	15:20	six	655	2270	626	2.02	elemental	5.67	1.00
3/31/03 15:22	15:42	inlet			619	2.00	elemental	4.64	0.26
3/31/03 16:01	16:20	inlet			583	1.88	total	7.33	0.15
3/31/03 16:21	16:40	one	654	2226	593	1.91	total	7.37	0.42
3/31/03 16:41	17:00	two	655	5029	592	1.91	total	2.92	0.38
3/31/03 17:01	17:21	three	655	2444	604	1.95	total	4.63	0.50
3/31/03 17:23	17:43	inlet			620	2.00	total	6.18	0.53
3/31/03 17:43	18:03	four	654	2403	603	1.94	total	5.40	0.28
3/31/03 18:03	18:23	five	654	2305	598	1.93	total	3.30	0.43
3/31/03 18:23	18:43	six	653	2092	613	1.98	total	5.49	1.05
3/31/03 18:46	19:06	inlet			398	1.28	total	7.48	0.27
4/1/03 8:37	8:57	inlet			660	2.13	total	7.48	0.68
4/1/03 8:57	9:17	one	657	693	700	2.26	total	9.50	0.22
4/1/03 9:17	9:38	two	657	4991	717	2.31	total	6.07	0.33
4/1/03 10:00	10:20	inlet			719	2.32	total	8.02	0.28
4/1/03 10:20	10:40	four	656	2399	744	2.40	total	4.90	0.49
4/1/03 10:40	11:00	five	656	2265	743	2.40	total	5.26	0.82
4/1/03 11:00	11:20	six	656	2305	736	2.37	total	4.56	0.53
4/1/03 11:22	11:39	inlet			549	1.77	total	7.97	0.11
4/1/03 14:58	15:18	inlet			1505	4.86	elemental	5.52	0.21
4/1/03 15:38	15:58	two	665	2431	1663	5.36	elemental	1.69	0.21
4/1/03 15:58	16:18	three	661	463	1572	5.07	elemental	1.70	0.25
4/1/03 16:21	16:40	inlet			1771	5.71	elemental	4.16	0.46
4/1/03 16:41	17:01	four	657	1218	1516	4.89	elemental	0.69	0.19
4/1/03 17:01	17:21	five	649	1210	1402	4.52	elemental	0.82	0.21
4/1/03 17:21	17:41	six	649	921	1518	4.90	elemental	1.41	0.42
4/1/03 17:43	18:03	inlet			1557	5.02	elemental	4.76	0.85
4/1/03 18:03	18:23	two	656	2482	1312	4.23	total	6.94	0.77
4/1/03 18:24	18:43	four	659	1134	1397	4.51	total	6.82	0.50
4/1/03 18:46	19:06	inlet			883	2.85	total	8.35	0.35

Start Time	End Time	Chamber	Tcab-avg, °F	SV, hr ⁻¹	NH ₃ , ppm	NH ₃ /NO	Species	Hg, ug/dscm	Hg St. Dev.
4/2/03 9:09	9:29	inlet			599	1.93	elemental	6.55	0.98
4/2/03 9:30	9:49	one	663	2064	0		elemental	6.31	0.51
4/2/03 9:50	10:10	two	661	5051	0		elemental	2.57	0.75
4/2/03 10:10	10:30	three	661	2439	0		elemental	0.99	0.28
4/2/03 10:32	10:52	inlet			0		elemental	5.98	0.76
4/2/03 10:52	11:12	four	659	2353	0		elemental	1.03	0.59
4/2/03 11:12	11:32	five	661	2132	0		elemental	1.72	0.99
4/2/03 11:32	11:53	six	662	2219	0		elemental	1.41	0.21
4/2/03 11:55	12:15	inlet			595	1.92	elemental	5.59	0.60
4/2/03 12:41	13:00	inlet			357	1.15	elemental	4.77	0.47
4/2/03 13:01	13:21	one	666	3580	357	1.15	elemental	4.95	0.24
4/2/03 13:21	13:41	two	666	8389	354	1.14	elemental	3.84	0.25
4/2/03 13:41	14:01	three	667	3921	362	1.17	elemental	5.63	0.23
4/2/03 14:01	14:21	four	667	3992	360	1.16	elemental	2.31	0.24
4/2/03 14:22	14:41	five	667	4571	362	1.17	elemental	5.79	0.25
4/2/03 14:42	15:01	six	668	3915	360	1.16	elemental	4.36	0.41
4/2/03 15:04	15:24	inlet			362	1.17	elemental	4.86	0.54
4/2/03 15:26	15:46	inlet			360	1.16	total	6.47	0.35

Table C.2. Averaged mercury data from second test series.

Date	Start	End	Chamber - Species	Tcat-avg, °F	SV, hr ⁻¹	NO _x , ppm (5%O ₂ , wet)	NH ₃ , ppm	NH ₃ /NO	Hg, dscm	Hg St.Dev
8/7/2003	14:55	15:24	Inlet - Total						7.07	1.33
8/7/2003	15:30	15:45	one - Total	590					6.82	1.14
8/7/2003	18:40	19:07	Inlet - Total						9.83	1.54
8/7/2003	19:24	19:57	Inlet - Total						9.34	2.27
8/7/2003	20:36	21:37	Inlet - Element						5.50	1.44
8/8/2003	8:46	9:30	Inlet - Total						6.51	0.37
8/8/2003	10:31	11:07	Inlet - Total						4.89	1.38
8/11/2003	12:39	13:08	Inlet - Total			335	357	1.07	5.89	0.43
8/11/2003	15:21	16:26	three - Total	599	2,587		336	1.01	4.47	0.37
8/11/2003	16:44	17:13	one - Total	555	2,958		338	1.01	3.72	0.60
8/11/2003	17:42	18:11	three - Total	600	2,599	83	337	1.01	6.51	0.08
8/11/2003	18:36	19:05	two - Total	554	5,687	94	341	1.02	6.60	0.34
8/11/2003	19:16	19:56	one - Total	555	2,745	307	342	1.02	7.36	0.27
8/11/2003	20:03	20:32	Inlet - Total			334	349	1.04	6.33	0.39
8/11/2003	21:36	22:01	four - Total	603	4,169	66	340	1.02	6.99	0.17
8/12/2003	13:27	13:44	Inlet - Element			347	371	1.07	4.19	0.06
8/12/2003	13:54	14:36	Inlet - Total			322	372	1.15	6.26	0.41
8/12/2003	14:53	15:16	one - Elemental	602	1,406	333	350	1.05	6.09	0.28
8/12/2003	15:35	16:05	three - Elemental	652	2,583	94	320	0.97	3.17	0.10
8/12/2003	16:18	17:02	two - Elemental	570	3,568	77	399	1.20	3.75	0.27
8/12/2003	17:15	18:03	Inlet - Element			335	396	1.18	4.11	0.32
8/12/2003	18:26	18:50	four - Elemental	605	2,541	83	395	1.19	4.41	0.63
8/12/2003	19:33	20:00	five - Elemental	543	3,635	92	394	1.19	3.02	0.09
8/12/2003	20:17	20:54	six - Elemental	555	2,219	118	405	1.22	4.03	0.31
8/12/2003	21:04	21:41	Inlet - Element			333	389	1.17	4.32	0.43
8/12/2003	21:48	22:15	Inlet - Total			321	385	1.20	4.25	0.41
8/13/2003	10:51	11:08	Inlet - Total			311	300	0.96	5.89	0.32
8/13/2003	11:18	12:05	Inlet - Element			310	297	0.96	5.04	0.41
8/13/2003	12:25	12:45	one - Elemental	553	1,803	309	299	0.94	4.79	0.26
8/13/2003	13:02	13:22	three - Elemental	591	2,587	113	292	0.92	4.32	0.34
8/13/2003	13:32	13:46	five - Elemental	547	4,564	108	295	0.92	3.07	0.08
8/13/2003	14:06	14:23	Inlet - Element			331	301	0.91	4.90	0.46
8/13/2003	14:30	15:17	Inlet - Total			313	300	0.96	4.84	0.39
8/13/2003	15:30	16:00	four - Elemental	615	2,669	115	290	0.91	5.02	0.38
8/13/2003	16:14	16:54	six - Elemental	566	2,314	133	298	0.93	5.91	0.71
8/13/2003	17:08	17:24	two - Elemental	553	4,841	121	296	0.93	5.32	0.07
8/13/2003	17:38	18:05	Inlet - Element			331	313	0.95	4.94	0.48
8/13/2003	18:15	18:35	Inlet - Total			318	313	0.98	4.99	0.54
8/15/2003	12:07	12:31	Inlet - Total			373	0	0.00	5.05	0.33
8/15/2003	12:39	13:03	Inlet - Element			380	0	0.00	3.29	0.33
8/15/2003	13:20	13:44	one - Elemental	581	455	431	0		3.19	2.73
8/15/2003	13:57	14:10	one - Elemental	582	110	410	0		3.18	1.86
8/15/2003	14:44	15:50	three - Elemental	636	2,584	428	0		3.79	1.92

Date	Start	End	Chamber - Species	Tcat-avg, °F	SV, hr ⁻¹	NO _x , ppm (5%O ₂ , wet)	NH ₃ , ppm	NH ₃ /NO	Hg, dscm	Hg St.Dev
8/15/2003	16:04	16:39	two - Elemental	586	3,976	424	0		2.85	0.81
8/15/2003	17:06	18:04	six - Elemental	576	2,251	476	0		6.12	4.90
8/15/2003	20:27	21:19	Inlet - Element			345	0	0.00	5.96	0.78
8/15/2003	21:24	21:48	Inlet - Total			330	0	0.00	6.29	0.38
8/15/2003	22:14	22:27	Inlet - Element			319	0	0.00	6.54	0.58
8/15/2003	22:35	22:53	two - Elemental	554	5,101	332	0	0.00	4.44	1.12
8/15/2003	22:57	23:14	two - Elemental	543	5,125	97	407	1.23	6.04	1.00
8/16/2003	10:33	11:41	Inlet - Element			309	350	1.13	5.24	0.25
8/16/2003	12:46	13:26	Inlet - Element			389	316	0.81	3.73	0.58
8/16/2003	16:33	17:08	three - Elemental	631	3,715	55	369.9	1.06	1.23	0.41
8/16/2003	17:31	18:10	five - Elemental	604	6,973	112	412.2	1.18	2.83	0.19
8/16/2003	18:16	19:53	five - Elemental	544	2,593	144	1308	3.75	4.89	0.53
8/16/2003	19:59	20:32	five - Elemental	540	2607	319.85	0		4.47	1.96
8/16/2003	20:39	20:56	five - Elemental	574	1112	343.47	0	0.00	3.59	1.89
8/16/2003	21:01	21:58	three - Elemental	573	1,115	148	1200	3.44	9.12	0.84